ARO 29044.1-MS-SBI

②

LASER COATING OF COMPOSITES FOR ENHANCED WEAR AND CORROSION RESISTANCE

Final Report for SBIR, Phase I Research
July 1, 1991 through December 31, 1991
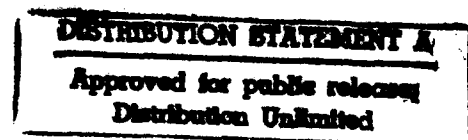
Contract No. DAAL 03-91-C-0040

Prepared for:

Strategic Defense Initiative Organization

Monitored by:

U.S. Army Research Office
P.O. Box 12211
Research Triangle Park
North Carolina 27709-2211

LASER SCIENCE COMPANY
ISIS Center, Suite 603
2501 North Loop Drive
Ames, IA 50010-8283

92 4 27 530

REPORT DOCUMENTATION PAGE

1. AGENCY USE ONLY (Leave blank)	2. REPORT DATE Jan. 28, 1992	3. REPORT TYPE AND DATES COVERED

4. TITLE AND SUBTITLE
LASER COATING OF COMPOSITES FOR ENCHANCED WEAR AND CORROSION RESISTANCE

5. FUNDING NUMBERS
DAAL03-91-C-0040

6. AUTHOR(S)
Madhav Rao Govindaraju, Arul Molian, P. Molian

7. PERFORMING ORGANIZATION NAME(S) AND ADDRESS(ES)
Laser Science Company
ISIS Center, #603, ISU Research Park
2501 North Loop Drive
Ames, IA 50010-8283

8. PERFORMING ORGANIZATION REPORT NUMBER

9. SPONSORING/MONITORING AGENCY NAME(S) AND ADDRESS(ES)
U. S. Army Research Office
P. O. Box 12211
Research Triangle Park, NC 27709-2211

10. SPONSORING/MONITORING AGENCY REPORT NUMBER
ARO 29044.1-MS-SBI

11. SUPPLEMENTARY NOTES
The view, opinions and/or findings contained in this report are those of the author(s) and should not be construed as an official Department of the Army position, policy, or decision, unless so designated by other documentation.

12a. DISTRIBUTION/AVAILABILITY STATEMENT
Approved for public release; distribution unlimited.

12b. DISTRIBUTION CODE

13. ABSTRACT (Maximum 200 words)

A new technique has been developed to produce glassy surface coatings on Metal Matrix Composites (MMCs) based on laser induced chemical reduction of metal salts. The substrate is first coated with a paste containing concentrated salts of the elements to be coated (ex. nickel formate, cobalt acetate, phosphorous, etc.) along with a thickening agent. The rise in the surface temperatures during laser irradiation will lead to the decomposition of salts to their native metals. The combination of these metal and metalloid elements in the reaction zone form an amorphous layer due to the specific chemical ratio and rapid cooling rate. The thickness of the coatings obtained were on the order of 50-100 microns, exhibited amorphous and microcrystalline structures, possessed hardness in the range of 300-1700 HV (substrate hardness 80-90 HV), and had superior. sliding wear resistance and excellent corrosion resistance. The formation of glassy surface coatings depends on the specific ratio of the metal-metal or metal- metalloids in the surface layers. The advantages of this process include the formation of glassy coatings on MMCs by a simple, versatile, technique which does not require any vacuum or inert atmospheres.

14. SUBJECT TERMS
Lasers, Coatings, Composites, Wear, Corrosion

15. NUMBER OF PAGES
43

16. PRICE CODE

17. SECURITY CLASSIFICATION OF REPORT	18. SECURITY CLASSIFICATION OF THIS PAGE	19. SECURITY CLASSIFICATION OF ABSTRACT	20. LIMITATION OF ABSTRACT
UNCLASSIFIED	UNCLASSIFIED	UNCLASSIFIED	UL

GENERAL INSTRUCTIONS FOR COMPLETING SF 298

The Report Documentation Page (RDP) is used in announcing and cataloging reports. It is important that this information be consistent with the rest of the report, particularly the cover and title page. Instructions for filling in each block of the form follow. It is important to *stay within the lines* to meet *optical scanning requirements*.

Block 1. Agency Use Only (Leave blank).

Block 2. Report Date. Full publication date including day, month, and year, if available (e.g. 1 Jan 88). Must cite at least the year.

Block 3. Type of Report and Dates Covered. State whether report is interim, final, etc. If applicable, enter inclusive report dates (e.g. 10 Jun 87 - 30 Jun 88).

Block 4. Title and Subtitle. A title is taken from the part of the report that provides the most meaningful and complete information. When a report is prepared in more than one volume, repeat the primary title, add volume number, and include subtitle for the specific volume. On classified documents enter the title classification in parentheses.

Block 5. Funding Numbers. To include contract and grant numbers; may include program element number(s), project number(s), task number(s), and work unit number(s). Use the following labels:

C	-	Contract	PR	- Project
G	-	Grant	TA	- Task
PE	-	Program Element	WU	- Work Unit Accession No.

Block 6. Author(s). Name(s) of person(s) responsible for writing the report, performing the research, or credited with the content of the report. If editor or compiler, this should follow the name(s).

Block 7. Performing Organization Name(s) and Address(es). Self-explanatory.

Block 8. Performing Organization Report Number. Enter the unique alphanumeric report number(s) assigned by the organization performing the report.

Block 9. Sponsoring/Monitoring Agency Name(s) and Address(es). Self-explanatory.

Block 10. Sponsoring/Monitoring Agency Report Number. *(If known)*

Block 11. Supplementary Notes. Enter information not included elsewhere such as: Prepared in cooperation with...; Trans. of...; To be published in.... When a report is revised, include a statement whether the new report supersedes or supplements the older report.

Block 12a. Distribution/Availability Statement. Denotes public availability or limitations. Cite any availability to the public. Enter additional limitations or special markings in all capitals (e.g. NOFORN, REL, ITAR).

DOD - See DoDD 5230.24, "Distribution Statements on Technical Documents."
DOE - See authorities.
NASA - See Handbook NHB 2200.2.
NTIS - Leave blank.

Block 12b. Distribution Code.

DOD - Leave blank.
DOE - Enter DOE distribution categories from the Standard Distribution for Unclassified Scientific and Technical Reports.
NASA - Leave blank.
NTIS - Leave blank.

Block 13. Abstract. *Include a brief (Maximum 200 words)* factual summary of the most significant information contained in the report.

Block 14. Subject Terms. Keywords or phrases identifying major subjects in the report.

Block 15. Number of Pages. Enter the total number of pages.

Block 16. Price Code. Enter appropriate price code *(NTIS only)*.

Blocks 17. - 19. Security Classifications. Self-explanatory. Enter U.S. Security Classification in accordance with U.S. Security Regulations (i.e., UNCLASSIFIED). If form contains classified information, stamp classification on the top and bottom of the page.

Block 20. Limitation of Abstract. This block must be completed to assign a limitation to the abstract. Enter either UL (unlimited) or SAR (same as report). An entry in this block is necessary if the abstract is to be limited. If blank, the abstract is assumed to be unlimited.
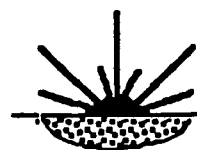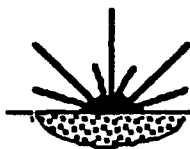
TABLE OF CONTENTS

ACKNOWLEDGEMENTS

1. INTRODUCTION

Metal-matrix composites (MMCs) are emerging as the most versatile materials for advanced structural, automotive, aviation and aerospace applications. These are composite materials consisting of a metal matrix, especially one with a low density and metallic or ceramic reinforcements in various forms such as, whiskers, particulates or fibers. Research efforts have involved developing aluminum-, copper-, magnesium-, titanium-, and lead-based MMCs, but the primary emphasis has been on developing aluminum-based composites. Reinforcements include graphite (Gr), silicon carbide (SiC), boron (B), or aluminum oxide (Al_2O_3). Fabrication techniques for these composites include chemical vapor deposition (CVD) coatings of the fibers, liquid-metal infiltration, powder metallurgy techniques, direct casting to near net shape and sqeeze casting.

Due to their high strength-to-weight ratio, high toughness, formability MMCs have been investigated for use in antenna and aircraft support structures, tarpedo and automobile engine pistons, aircraft vertical tail fins, and initial guidance and precision optical systems (1). Composites of boron/Al is used as cargo bay stiffners on the space shuttle (2).

However, there exists a need to protect these various types of composites used in space structures from corrosion, oxidation and wear. Although vapor deposition techniques may be used to deposit protective coatings to minimize the tribological and environmental problems, the need for the vacuum will not permit these techniques to be used on large scale structures. Other methods such as electroless plating are tedious and not versatile. An innovative process is required to deposit protective coatings for composite structures without complexity. A laser glazing method has been proposed to deposit refractory amorphous coatings on composite surfaces and thereby provide the required protection.

Amorphous or glassy metal coatings are single-phase alloys with short-range order of atoms which can be made by very rapid solidification of certain metal-metalloid or metal-metal melts. These supercooled glassy metals possess remarkable combination of properties as a result of their unusual atomic structures. Such properties include strength, hardness, ductility, toughness, corrosion resistance, electrical resistivity and magnetic permeability (3).

Glassy alloys can be produced from two or more transition metals, for example, Cu-Zr, Ni-Nb, Ti-Be, Ca-Mg with 50:50 in composition. In the metal-metalloid group, typical glass forming compositions are 80 at% late transition metals, such as Fe, Co, Ni, Pd, Au containing 20% metalloids, such as B, C, si, P and Ge (4).

Melt spinning is the usual method of producing glassy metals, yielding 20-60 microns thick, 1-20 mm wide ribbons. Because of the need

1
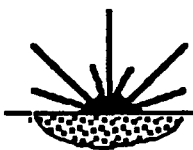
for extremely rapid quench rates, glassy metals are often produced in the form of ribbons, wires and filaments (5). The second set of techniques to form glassy metals involves growth from the vapor phase, such as sputtering, or from a liquid phase, such as electroless deposition or electrodeposition. By virtue of their higher effective cooling rates these techniques allow the formation of glassy metal that cannot be produced by splat quenching. Other methods of producing glassy metals include ion implantation, ion-beam mixing, irradiation by high energy density beam such as laser or electron beam.

2. Phase I Project Objectives

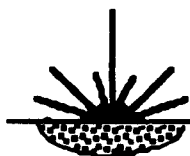The technical objectives of Phase I research are:

1. To produce glassy refractory protective coatings on metal matrix composite surfaces by a laser glazing technique.

2. To develop a methodology of evaluating the quality of the coatings by eddy current NDE technique.

The project is aimed to enhance the corrosion, oxidation and wear resistance of composites used in aerospace, automobile and space applications.

2.1 Laser Glazing Technique

Lasers are increasingly used in many surface engineering applications. The emergence of laser as a tool for materials development and/or processing can be attributed to its characteristics such as, localized heat source, inertialess beam, highly controllable power density, short interaction time and chemical cleanliness. The variations in laser power density and interaction time have resulted in several materials processing operations such as transformation hardening, surface alloying, surface cladding and laser glazing (6).

Laser glazing process (Figure 1) consists of melting a localized thin surface layer in intimate contact with a cold, solid substrate using a laser beam of high power density (10^5 - 10^8 W/cm^2) and short pulse time (10^{-5} - 10^{-8} sec). Rapid surface melting occurs in a time during which little thermal energy penetrates into the base material. This leads to the development of extremely high thermal gradients, which promote rapid solidification of the metal. Cooling rates of the order of 10^6 - 10^8 °C S^{-1} can be achieved which results in metastable microstructures with epitaxial growth. The solidification starts at the melt layer/substrate interface and progresses towards the surface with continued cooling. The interface remains in an equilibrium state, while the material above it solidifies dendritically at a high quench rate (7). In special cases, amorphous solidification can occur with the suppression of crystallization.

LASER BEAM →

45° ANGLE
MIRROR

LENS

SHIELD

INERT GAS

SPECIMEN

ROTATING DISC

VARIBLE
SPEED
MOTOR
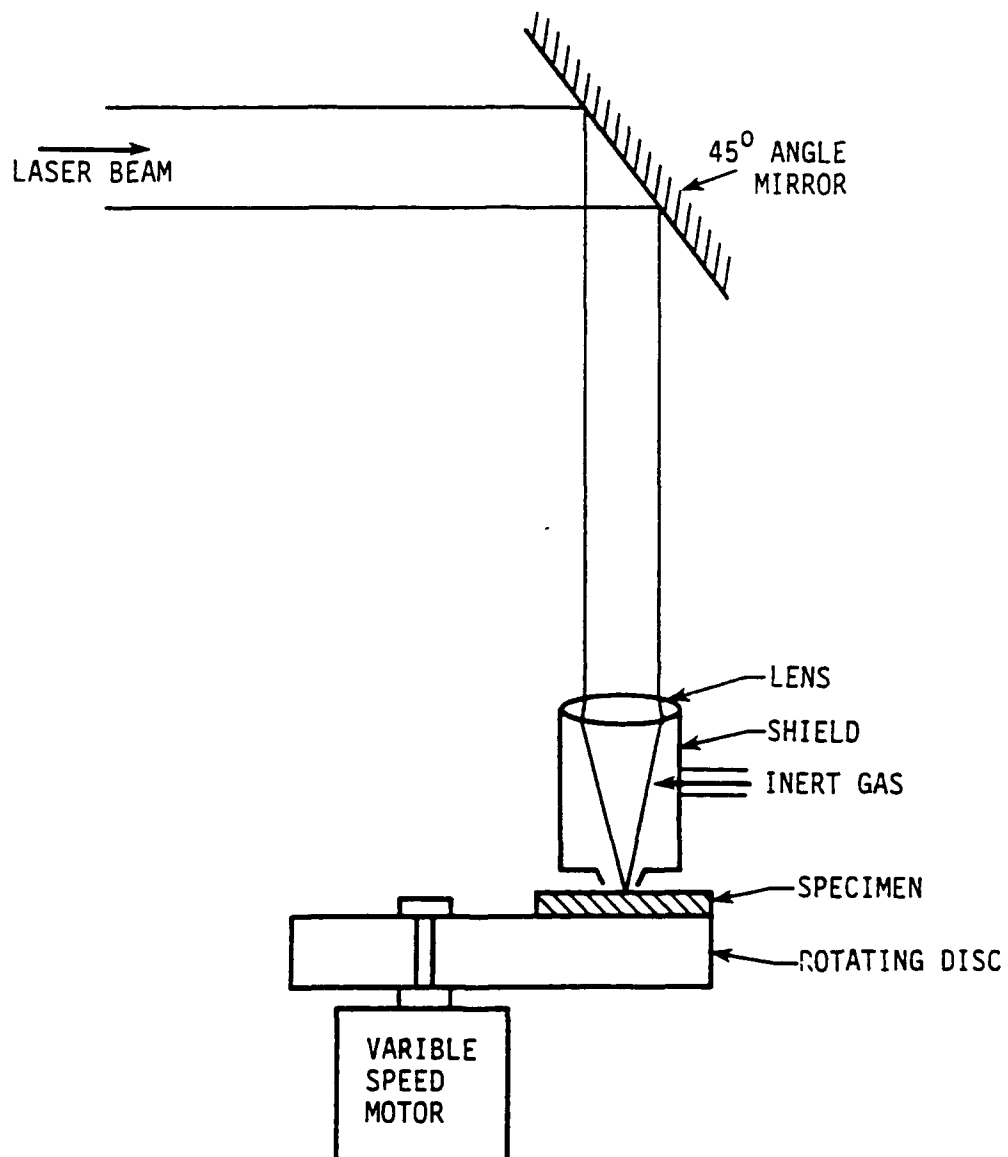
Figure 1. Schematic of Laser Glazing Process
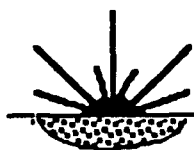
In Phase I work, we have extended the laser glazing technique to apply metallic glass refractory coatings on metal matrix composites.

3. EXPERIMENTAL DETAILS

3.1 Lasers used in the Investigation

A 1.5 kW (nominal) CO_2 laser was mostly used to conduct laser glazing studies. The other lasers used include Nd:YAG and excimer (ArF). The specifications of these lasers are listed in Table 1. CO_2 lasers yielded better results because of their high power, better beam profile and small divergence. It should be added that a low-divergence type laser such as CO_2 is ideal for accurate and reproducible results. All three lasers were initially used in pulsed mode because of their capability to produce glassy structures by providing high power density and short interaction time. However, it was very difficult to achieve uniform surface coverage with a pulsed system, because of the need for precise coordination between the scanning and pulsing systems. Another problem was the nonuniform energy profile within each pulse. Although Nd:YAG laser generated higher energy density in pulsed mode than CO_2 laser, the Nd:YAG's poor beam quality (multimode) did not provide satisfactory results. Experiments with continuous wave lasers were successful. Between Nd:YAG and CO_2 continuous wave lasers, CO_2 laser was better due to its high power and better beam quality.
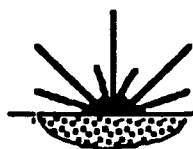
Table 1. Specifications of the Lasers Used in the Investigation

	Nd:YAG (Pulsed)	(CW)	CO_2 (CW/Pulsed)	Excimer ArF(Pulsed)
Average power, kW	0.4	0.1	1.5	0.05
Wavelength, nm	1060	1060	10,600	193
Peak power, kW	12	0.1	5	20,000
Pulse time	msec	-	msec	nsec
Repetition rate, Hz	1-200	-	1-100	1-100
Beam quality	Multimode	Multimode	Gaussian	Multimode

3.2 Specifications of Substrates

The substrates used in this investigation were aluminum based metal matrix composites (MMCs) reinforced with silicon carbide particles. These were obtained from DURALCAN USA, Division of Alcan Aluminum Corporation, San Diego, California. The samples were sand cast Duralcan F3A.10S and Duralcan F3A.20S (general purpose composites) which contains 10 and 20 volume % of silicon carbide particles respectively. The discontinuous particles ranged in size from 15 to 50 microns.

The nominal composition of matrix (A356) was 7 Si, 0.2 Fe, 0.20 Cu, 0.10 Mn, 0.35 Mg, 0.10 Zn, 0.20 Ti, balance aluminum (all in weight

%). The dimensions of samples were 15 mm X 40 mm X 6 mm, which were mechanically polished to a random finish with 320 grit SiC paper. Samples were then cleaned thoroughly with water and in methanol prior to laser treatment.

3.3 Selection of Coatings

Various coating materials including metallic glass ribbons, pure metals, oxides and complex salts were used. The coatings prior to laser glazing were applied by various methods such as: (i) bonding glassy ribbon to the composite substrate, (ii) pre-placing powders of pure metals and oxides, (iii) electroless plating of Ni-P deposits and (iv) covering the surface with jellies containing concentrated salts of the elements to be coated.

The amorphous glassy ribbons used in the study were (i) Co-Cr-W-B (METGLAS MHF 157), (ii) Ti-Zr-Cu-Ni (METGLAS MBF 5002), (iii) Co-Si-B (METGLAS 2714A) and (iv) Ni-P (METGLAS MBF 60). These glassy ribbons were commercially available from Allied Signal, Inc., New Jersey. The thickness of glassy foils were about 15 - 50 microns. The chemical compositions of glassy ribbons used are given in Table 2.

In the second method, pure metal powders (99.9 % purity) of cobalt and molybdenum, and zirconium oxide were preplaced on the substrate. In the third method, electroless plating of amorphous Ni-P on the substrate was carried out using the standard chemicals and procedures. These samples were subsequently subjected to laser beam irradiation.

Table 2. Chemical Composition of Glassy Ribbons

MHF 157		MBF 5002		2714A		MBF 60	
Co	Bal.	Ti	37.5	Co	66	C	0.10
Cr	21.0	Zr	37.5	Fe	4	P	11.00
W	4.5	Cu	15.0	Ni	1	Ni	BaL
Si	1.6	Ni	10.0	B	14		
B	2.4			Si	15		
C	0.07						

Finally, a novel method namely laser induced chemical reduction of metal salt precursors was attempted. In this process, the metal salt precursors were mixed with a thickening agent to enhance the viscosity of the solution. This viscous paste was applied on the substrate, dried and then irradiated by the laser.

3.4 Laser Coating Procedure

The composite substrates with pre-placed glass-forming alloys were irradiated with CO_2, YAG and excimer lasers in conjunction with
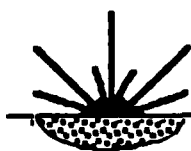
appropriate optical tools. A typical experimental set-up with CO_2 laser is shown in Figure 2. The Gaussian beam from the laser was made to oscillate bidirectionally by means of wobble rotation of a mirror (see Figure 2) and then focused through a lens to form an elliptical profile.

It can be noted that the size of ellipse may be increased by reducing the angle O and thereby providing increased coverage rate. The purpose of oscillating a focused Gaussian beam is to enhance the coverage zone. Typical widths of laser glazed zones, depending on the focal length of lens, were from 5 mm to 10 mm. The frequency of oscillation was made constant in this study and was equal to 1000 rpm.

Laser glazing experiments were conducted using three different focal length lenses: 63 mm, 127 mm and 188 mm. Best results were obtained with 127 mm focal length lens. The scan rate of laser beam is an important parameter and determines the interaction time of laser beam. The scan rates were varied from 4 to 254 mm/sec. For the oscillating beam set up, the scan rate was held less than 40 mm/sec because the frequency of oscillation (1000 rpm) was not high enough to allow continuous, uniform coverage. An argon shield gas was used to protect the lens during laser glazing.

In the oscillating Gaussian beam setup, the laser glazed width per scan was about 5 mm when 127 mm focal length lens was used. Multiple, overlapping scans were carried out to increase the width. For characterization and analysis purposes, a total of 3 scans with an overlapping of about 30 % for each sample was performed (see Figure 3b). For corrosion and wear test samples, a total of 20 scans was carried out. Figure 3 shows the top view and transverse section of multiple laser scan sample. Tempering always occurs in multiple laser scans.

4. RESULTS AND DISCUSSION

4.1 Laser Glazing of Glassy Metal Ribbons

In the first approach, melt spun ribbons of metallic glasses were attached to the substrate by using an adhesive. The substrate and the glassy metal ribbons were cleaned with methanol. The ribbons were cut to the same length as the substrate and attached to the substrate with their shining face down by using super glue. Initially two different types of adhesives, viz., crystal bond and silver epoxy were tried to attach the glassy ribbons. However, the samples with crystal bond as the adhesive medium resulted in dark, sooty appearance upon laser glazing and hence were rejected. Silver epoxy was also not very effective in attaching the metallic glass ribbons to the substrate. Eventually the ribbons were attached by using super glue.

The samples were irradiated by using all the lasers listed in Table 1. Microstructural analysis showed that the depths of laser affected layers were of the order of 200-300 microns. In the case of

RAW
BEAM

WOBBLE
ROTATION

MIRROR

MOTOR/PULLY
REDUCTION SETUP

θ

LENS

ELLIPTICAL
PROFILE

V

SPECIMEN
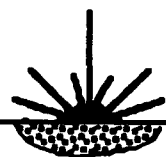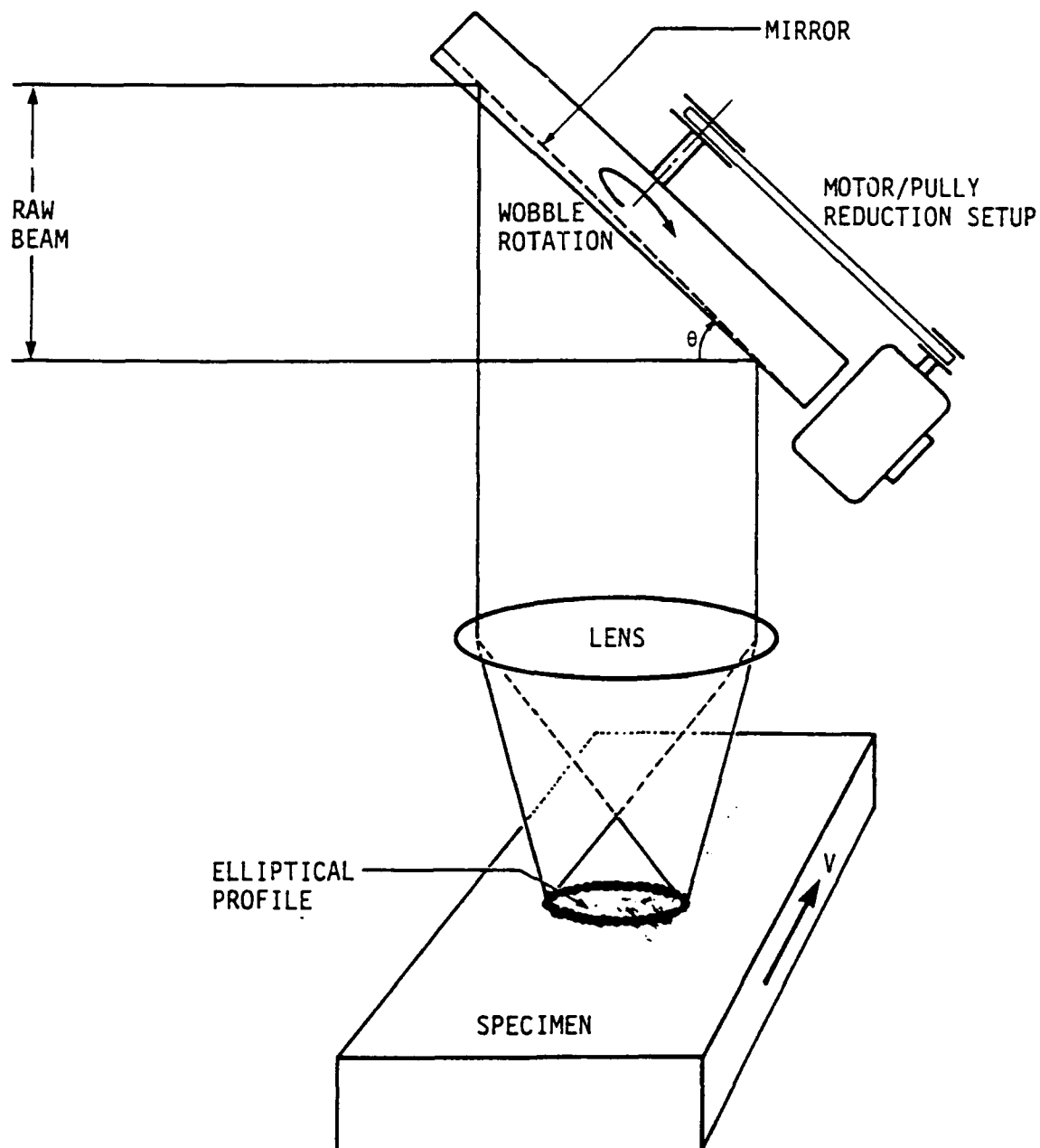
Figure 2. Schematic of Laser Glazing of Precoated Metal Matrix
Composites.
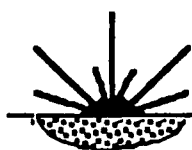
samples glazed with cobalt based glassy metal ribbons (METGLAS MHF 157 and 2714 A) there was no evidence of any glassy layer formation. The chemical analysis also showed the absence of any coating material on the substrate, except in occasional cases. This may be due to the instantaneous evaporation of glassy metal ribbons. This was confirmed from the experiments using the 50 watts CW Nd:YAG laser and 4 watts excimer laser. It was observed that the glassy metal ribbons were evaporating even at this lower powers with virtually no visible effect on the substrate.

Amorphous-like layers were formed by using glassy metal ribbons of Ti-Zr-Cu-Ni (METGLAS MBF 5002) under specific process conditions of higher glazing speeds of 125 mm/sec and 1250 watts power (Figure 4). However, these results could not be reproduced. Very promising results were also obtained using glassy metal ribbons of nickel-phosphorous (MBF 60), which also could not be reproduced.

The problems associated with the formation of amorphous coating using glassy metal ribbons may include:

* metallic glass ribbons virtually absorb all the laser power resulting in localized high energy density areas and giving rise to instantaneous vaporization of the main alloying elements

* lack of transfer of absorbed energy to the substrate at the interface due to poor adhesion of glassy ribbons to the substrate.

It should be added that reducing the power density to a very low level prevented the evaporation of glassy ribbons but did not melt the substrate because aluminum requires higher power density to initiate melting.

Although our approach yielded limited success, Hashimoto et al. and (8), Kumagai et al. (9) produced Pd-based amorphous surface alloys on nickel and nickel-plated substrates using a little different technique. This technique involved bonding the Pd-glassy ribbons on the substrate by spot welding and then heat treating under a vacuum of 10^{-7} torr until the ribbons were melted; subsequently, laser treatment was applied. This technique suffers from the drawbacks of melting the glassy ribbons prior to laser treatment, and high vacuum requirement.

### 4.2 Laser Glazing of Pure Metals, Oxides and Composite Powders

The samples with pre-placed powders of pure cobalt, molybdenum, zirconium oxide and composite powder consisting of nickel-chromium-aluminum-cobalt-yttria and yttria stabilized zirconia were irradiated by CW CO_2 laser operating in oscillating Gaussian beam at powers ranging from 500 - 1500 watts. Metallographic examination confirmed the
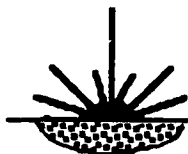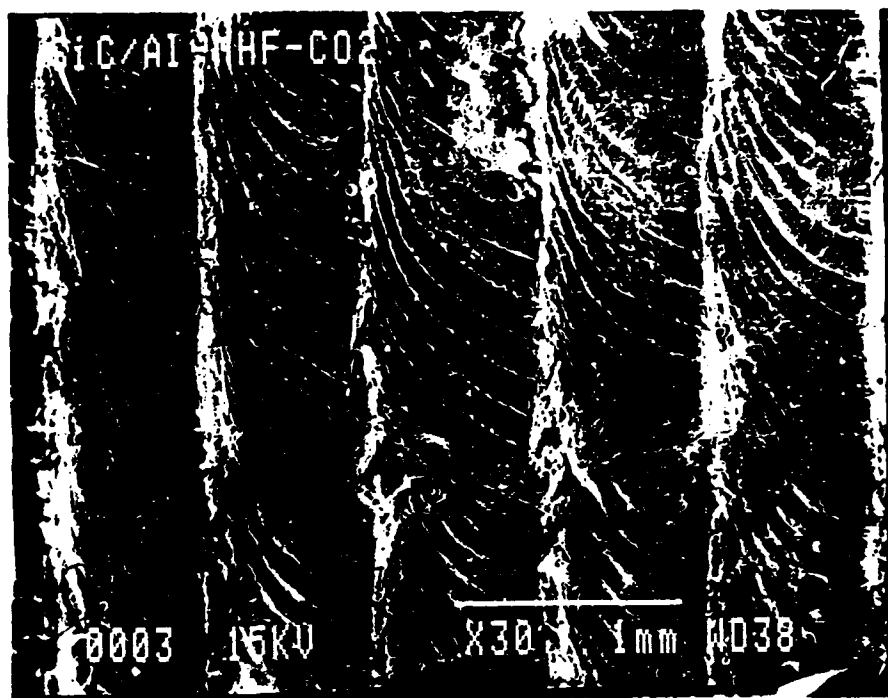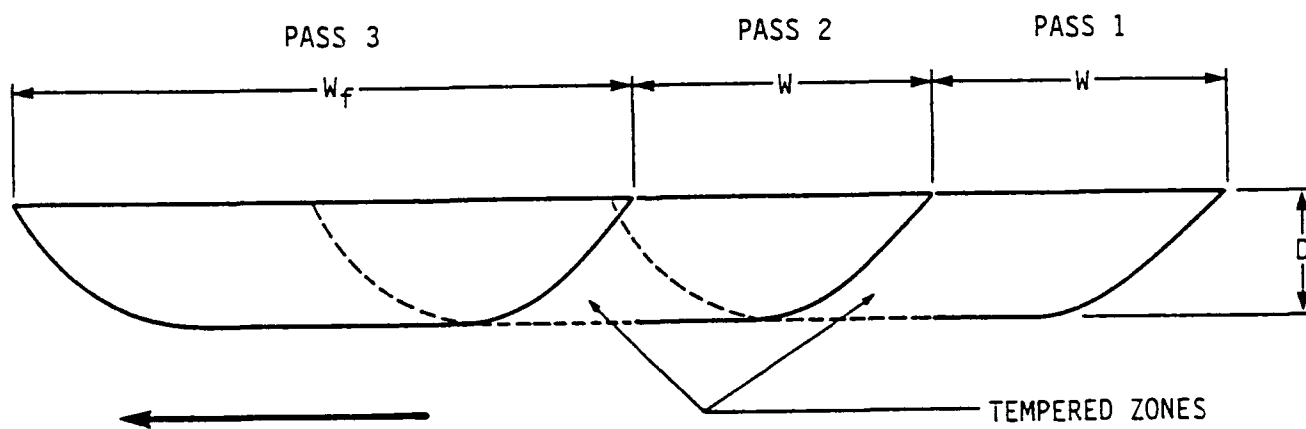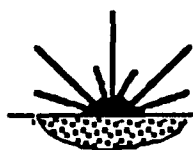
(b)

Figure 3. (a) Scanning electron micrograph showing the top view of laser glazed sample, (b) Schematic showing the transverse section of multiple overlapping laser scans.

feasibility of forming an amorphous layer in samples glazed with pre-placed cobalt powders. The laser glazed surfaces however, exhibited a rough surface finish with some discoloration. This roughness can be attributed to surface rippling effect. Evidence of amorphous-like layer formation, as seen in Figure 5, was observed only in scans processed at higher powers (1000 watts) and low scan rates (20 mm/sec). At further higher powers of 1500 watts, degradation of substrate was noted.

Laser glazing of other powders was not satisfactory. These studies indicate that the formation of amorphous layers using pre-placed powders was feasible only with certain chemical compositions and under specific process conditions.

4.3 Laser Glazing of Electroless Coatings of Ni-P

Electroless nickel coatings are often used in industrial applications because of their high resistance to wear and corrosion. The corrosion resistance is attributed to the amorphous nature and passivity of the coating. Laser treatment of the nickel-phosphorous layer is expected to improve the adherence. The Al/SiC samples were pretreated using a procedure given in Table 3 and then coated with Ni-P alloy by electroless method. Table 4 shows the composition of the immersion bath. Two samples were coated for 4 and 5 hours. The coated samples were then treated with CO_2 laser at various powers.

The laser glazing of electroless deposits produced only localized amorphous-like layers of the order of 50-60 microns, as shown in Figure 6, under the process conditions of 250 watts and a scan rate of 2 mm/sec.

4.4 Laser Chemical Reduction of Complex Metal Salts

In this newly developed process, amorphous surface layers can be formed by laser induced chemical reduction of metal salts. The surface of the substrate is first covered with a layer containing concentrated salts of the elements to be coated along with a thickening agent, such as agar. During subsequent laser irradiation, the rise in the surface temperatures will lead to decomposition of salts to native metals. These metals will be dissolved into the melted substrate and form amorphous layers due to the chemical composition and rapid cooling rate which is typical of the laser glazing process.

Initial experiments were conducted by applying precursors of nickel, cobalt, chromium and phosphorous. Phosphorous was used due to its well established capability of enhancing the formation of glassy metals. The selected metal salts were Nickel formate (Ni), Cobalt acetate (Co), Chromium chloride (Cr) and Phosphorous oxide (P). Three different compositions of complex salts were evaluated for the formation of amorphous layers,(i) 65% Nickel formate - 30% Phosphorous pentoxide,(ii) 35% Nickel formate - 35% Cobalt acetate - 25% Phosphorous pentoxide and (iii) 25% Nickel formate - 25% Cobalt acetate - 25%
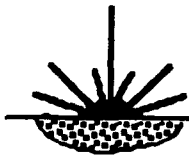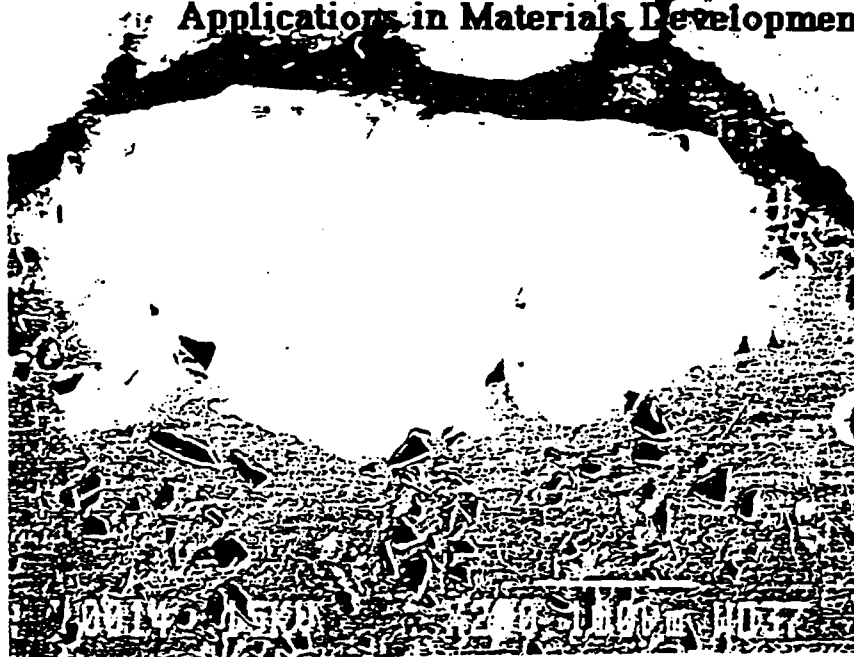
Figure 4. Scanning electron micrograph of laser glazed Al/SiC adhesive bonded with Ti-Zr-Cu-Ni metallic glass ribbon (METGLAS MBF 5002), showing an amorphous-like layer, Mag 200x.
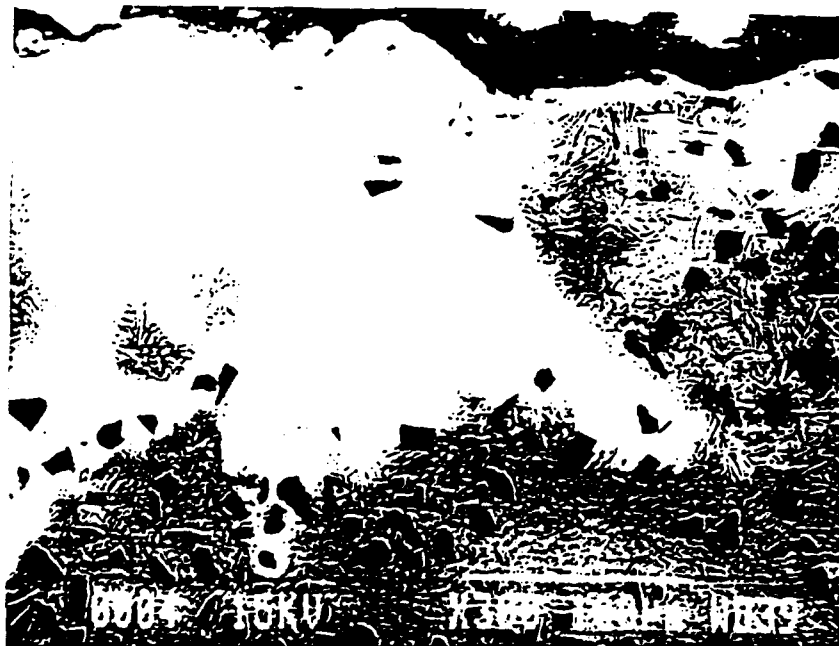

Figure 5. Scanning electron micrograph of laser glazed Al/SiC preplaced with cobalt powder showing amorphous-like layer, Mag.300x.
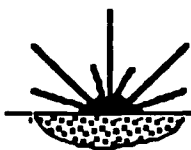
Table 3. Procedure used for pre-treatment of the samples before electroless plating.

1. Cleaning, Degreasing and Rinsing

2. Immersion in Sodium Hydroxide, 5% solution

3. Etching in:

    Nickel chloride, $NiCl_2.\ 6H_2O$.   140 g/l
    Orthophosphoric acid, H_3Po_4 1   g/l
    Temperature   40-50 ^oC
    Duration   10-20 sec.

4. Immersion in concentrated HNO_3 for 2-3 minutes.

5. Immersion in:
    Mixture of HNO_3 and HF acid.
        8N HNO_3
        48% HF
        15-45 sec.

6. Repeat steps 3-5.

Table 4. Composition of the electroless bath

Nickel chloride, $NiCl_2.6H_2O$ 30g

Sodium Hypophosphite,
    $NaH_2PO_2.H_2O$ 10g

Sodium Hydroxyacetate   50g
    $HO\ CH_2COONa$
Base   NaOH
pH   4-6
Water   1L
Speed of separation (Approx) 15 microns/hour
Temperature 90^oC
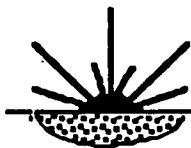
Chromium chloride - 20% Phosphorous pentoxide (all % are weight percentages). A 5 wt % thickening agent, agar-agar gum, was added to enhance the viscosity of the solution. The samples were then treated with (i) Nd:YAG with powers of 50 (CW) and 400 watts (pulsed), (ii) Excimer laser (ArF) with power of 4 watts and (iii) CO_2 lasers with powers ranging from 250 - 1250 watts under varying process conditions. The effect of laser power and specimen scanning rate on the capability of forming metallic glass layers was investigated.

It was observed that the use of Nd:YAG at 50 watts (CW) and 400 watts (pulsed), excimer laser at 4 watts and CO_2 laser at 250 watts did not have any significant reaction with metal salt precursors. This may be due to low temperatures generated during laser irradiation which are insufficient to decompose the metal salts. Only the use of CO_2 laser at higher powers (500 watts and above) showed the formation of amorphous-like layers on the surface, as shown in Figures 7 and 8. Scanning electron microscopical examination shows the coating thickness to be on the order of 100 microns. Examination at higher magnifications did not reveal any crystalline structural features leading to the conclusion that the coating is amorphous.

These experiments involving laser chemical reduction of metal salts demonstrated the significant evidence of amorphous-like coating. This new process has the ability to form coatings of any complex composition desired. The relative compositions of metallic (chromium, nickel, cobalt, molybdenum, iron, etc.) or nonmetallic (boron, carbon, phosphorous, etc.) elements can be varied to enhance the formation of amorphous coatings. This new process has a great potential for novel technological applications due to the ease with which the metallic precursors can be deposited on the substrate. Also this method is well suited for scaling-up operation.

4.5 Further Studies of Laser Glazing Procedure Using Complex Salts

Due to the success of the laser chemical reduction of complex salts procedure in forming amorphous-like coatings, further work was concentrated on establishing the process variables, characterizing the structure, chemical composition and evaluating the corrosion and wear resistance of the coatings.

The compositions of metal salts used in the study were chosen which have the capability to form glassy structures. The chemical formulae along with their weight percentages of elemental metal contents are listed in Table 5. It is well known that glassy structures can be produced by rapid solidification of certain metal-metalloid or metal-metal melts. For example in metal-metal group, glassy metals can be produced from transition metals, such as Cu-Zr, Ni-Nb, Ti-Be, Ca-Mg with 50:50 in composition. In the metal-metalloid group, typical glass forming compositions are 80 at % transition metals, such as Fe, Co, Ni, Pd and Au and 20 at % metalloids, such as B, C, Si, P and Ge (5). Based
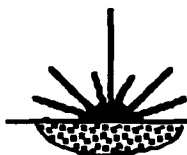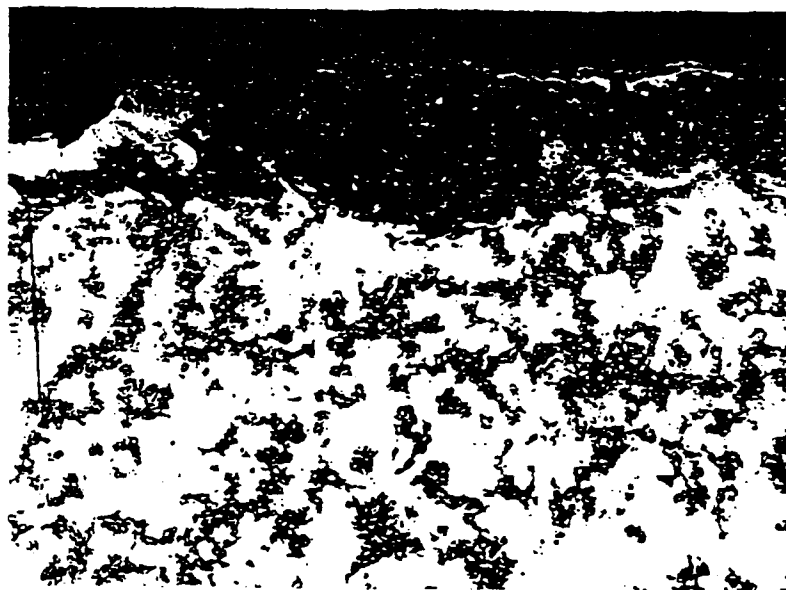
Figure 6. Optical micrograph of laser glazed Al/SiC predeposited with Ni-P (by electroless plating) showing localized amorphous-like regions (bright arreas), Mag. 100x.
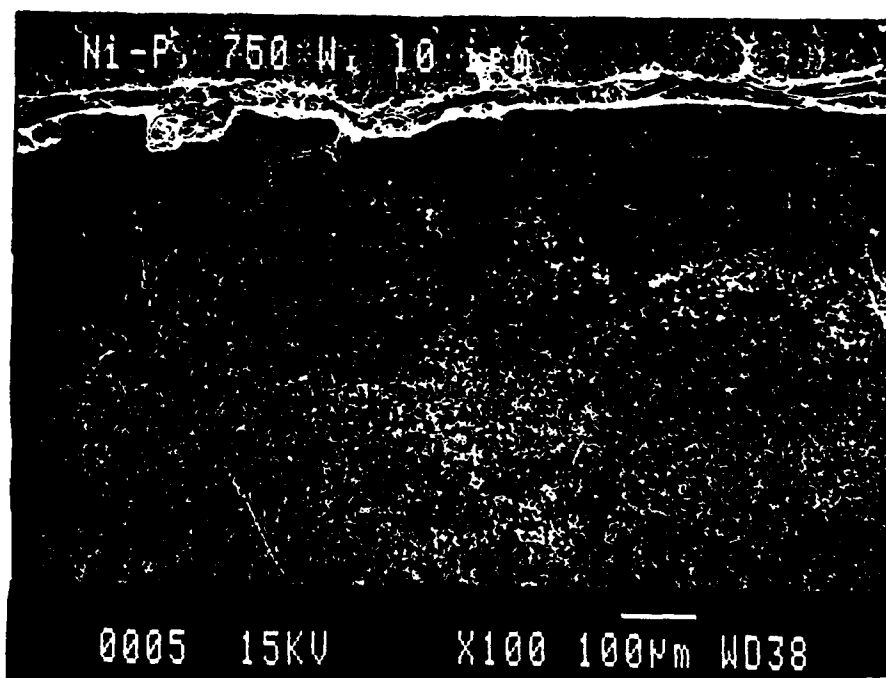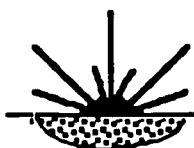

Figure 7. Scanning electron micrograph of laser glazed Al/SiC predeposited with nickel and phosphorous salts showing amorphous-like coating, Mag.100x.

on this information the precursor salts were proportioned to yield the following compositions of metals and metalloid:

1. 45 % Ni, 35 % Co, 20 % B

2. 35 % Ni, 25 % Co, 20% Cr, 20 % B

Table 5. Compositions of metal salts used in the investigation

Chemical Name	Formula	Formula Weight	Wt% Metal
Nickel Formate	$Ni(CHO_2)_2 \cdot 2H_2O$	184.71	31.70 (Ni)
Cobalt Acetate	$Co(CH_3COO)_2 \cdot 4H_2O$	249.08	23.66 (Co)
Chromium Chloride	$CrCl_3 \cdot 6H_2O$	266.45	19.51 (Cr)
Phosphorous Pentoxide	P_2O_5	141.94	43.68 (P)

The preparation process involved mixing the metal salts in the given proportion with water. A thickening agent (5-10 wt % agar-agar gum) was used to enhance the viscosity of the solution. The solution was heated at 100 - 120 °C for 10-15 minutes to evaporate water. The resulting thick paste was applied on the sample uniformly with a spatula. The thickness of the coating was on the order of 3 - 5 mm. In the second method, the salts were dissolved in methanol. The mixture was deposited on the substrate and heated to 60-80 °C for a few minutes and allowed to cool to obtain a solid precursor layer. In the third method, the salts were dissolved in polyethylene oxide (PEO). PEO is chosen because of its high transparency to laser light. Under these conditions, laser radiation heats effectively and thereby enhances the decomposition and incorporation of metals in the melt. However, results indicate that amorphous layers were produced better by using water. The substrates covered with a thick layer of metal salt precursors were irradiated by CO_2 laser. After laser exposure, the samples were thoroughly cleaned with water to remove the untreated precursors and resultant organic residues.

4.6 Metallography and Compositional Analysis

The laser coated specimens were sectioned perpendicular to the scan direction, mounted in epoxy, mechanically polished and etched for 8-12 seconds in Keller's etchant. The specimens were then examined by optical and scanning electron microscopy. Metallographic analysis showed the evidence of amorphous-like coating in the samples prepared with metal salt precursors of Ni, Co and B. Figures 9 and 10 show the
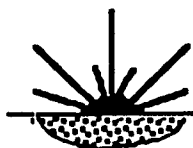
formation of amorphous-like coating on the samples glazed at laser powers of 1000 and 1500 watts respectively. Analysis at various locations on the samples confirmed the nature of coatings to be consistently amorphous-like, with coating thickness ranging from 50 - 70 microns. Microstructural examination of coatings even at higher magnifications did not reveal any specific structural features. WDAX showed the presence of Ni, Co, Si and Al in the coating. The presence of Al and Si in the coating shows the possibility of vigorous surface reaction between the metal salts and the composite substrate. There was no evidence of cracks or porosity in laser glazed layers.

The coating system has been modified to include Cr which is said to enhance the corrosion resistance of glassy materials (8). Figure 11 shows the micrographs of laser glazed Ni-Cr-Co-B coating system. X-ray energy spectrum (Figure 12) of the coated layer shows the presence of Ni, Cr, Co and the substrate elements. Figure 13 shows the uniform distribution of Ni, Cr and Co revealing the chemical homogeneity of the coating.

4.7 X-Ray Diffraction Analysis

The structural and compositional analysis of the laser-processed samples were analyzed by X-Ray diffraction method using Cu K-alpha radiation. The X-Ray diffraction patterns were obtained using Siemens D500/SRS 200. Figure 14 is the X-ray diffraction pattern of Al/SiC composite substrate showing sharp peaks associated with Al, Si and SiC. Figures 15 and 16, the X-ray diffractograms of laser glazed Ni-Co-B and Ni-Cr-Co-B coatings respectively, exhibit both diffused and sharp peaks characteristic of amorphous and crystalline structures. The crystalline phases were identified to be intermetallics that include nickel cobalt chromium (NiCoCr), aluminum carbide (Al_4C_3) and aluminum cobalt (Co_2Al_9) in addition to Al, Si and SiC. The intermetallic NiCoCr usually forms under rapid solidification conditions. We could not observe true glassy structures (X-ray patterns that exhibit broader and diffused peaks) because the coating consists of a mixture of amorphous and crystalline regions and the depth of X-ray penetration is larger than that of the coating thickness.

4.8 Microhardness Evaluation

Microhardness tests were conducted using a Vicker's diamond pyramid indenter at a load of 500 grams. The hardness of coating varied as a function of scan rate. Table 6 provides the hardness and glazed depth (coating thickness) of Ni-Cr-Co-B coatings. Hardness of the overlapping zones (250 - 300 HV) were lower than the single-scan zone (400 HV). The hardness was increased with a decrease in scan rate. The sample processed at a low scan rate 17 mm/sec consisted of soft and hard regions with hardness ranging from 300 to 1700 HV. High hardness regions did not exhibit any crystalline features. Figure 17 shows the hardness indentations on the substrate and the laser glazed zone. The small indentation regions appear to be amorphous-like.
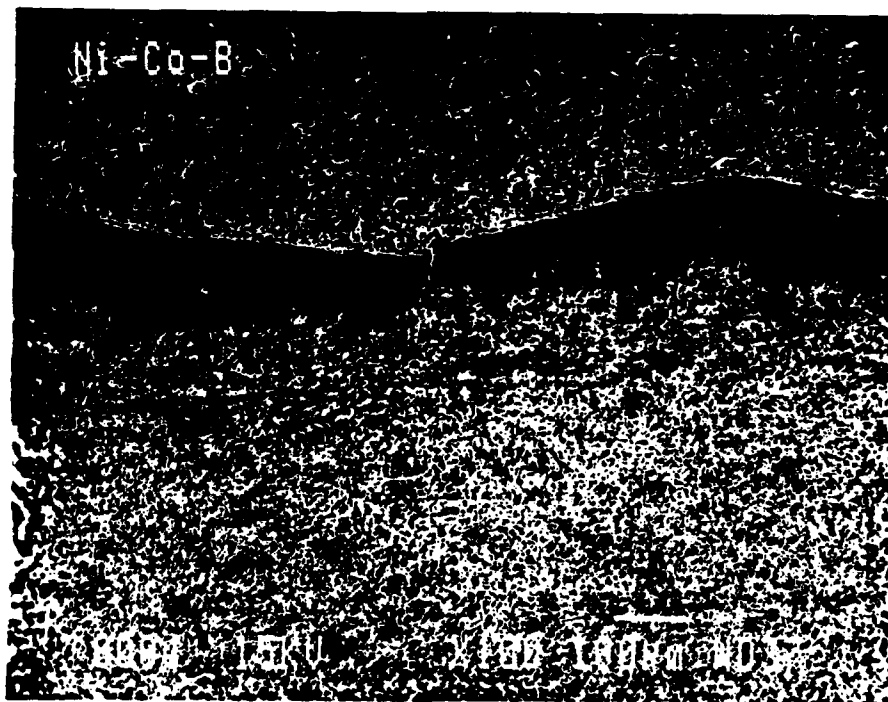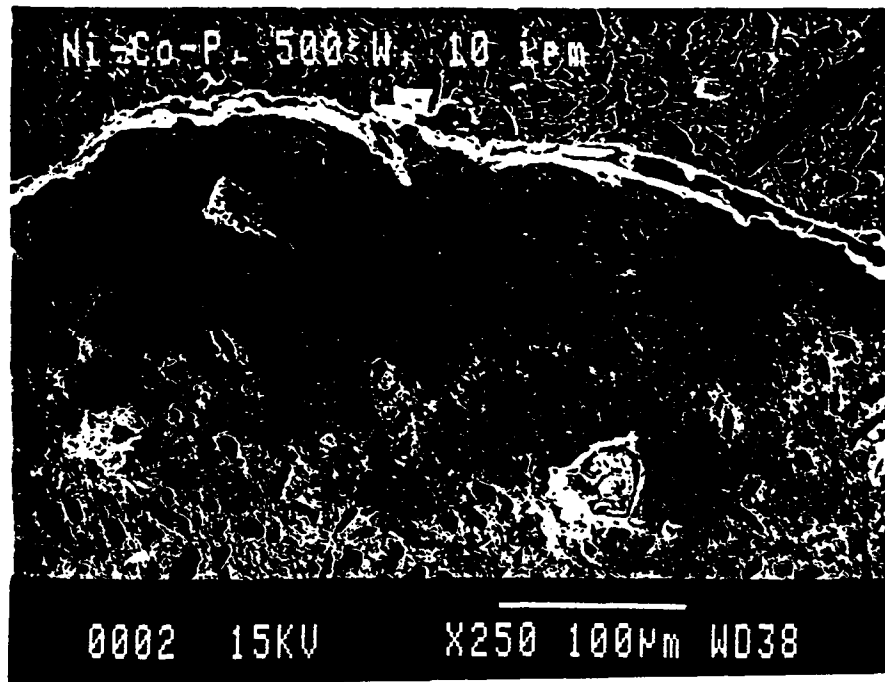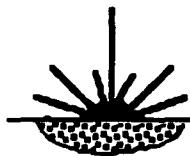
Figure 8. Scanning electron micrograph of laser glazed Al/SiC
predeposited with (a) nickel, cobalt and phosphorous salts, (b)
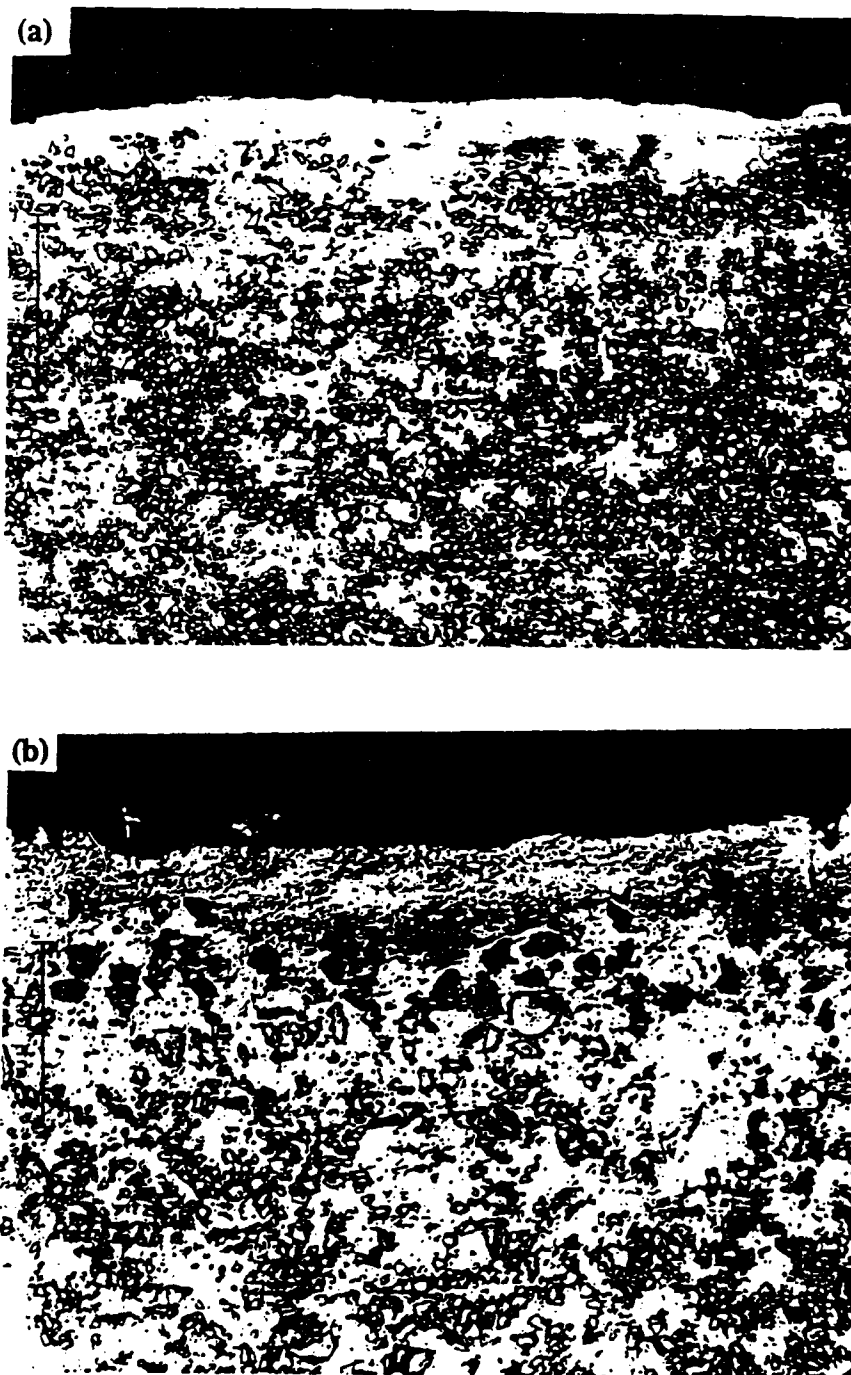nickel, cobalt and boron showing amorphous-like coating,
Mag.100x.

Figure 9. Optical micrographs of laser glazed Al/SiC predeposited with salt precursors of Ni, Co and B (Laser power 1000 watts) showing the uniform glassy-like layers. (a) Mag.100x, (b) Mag.250x.
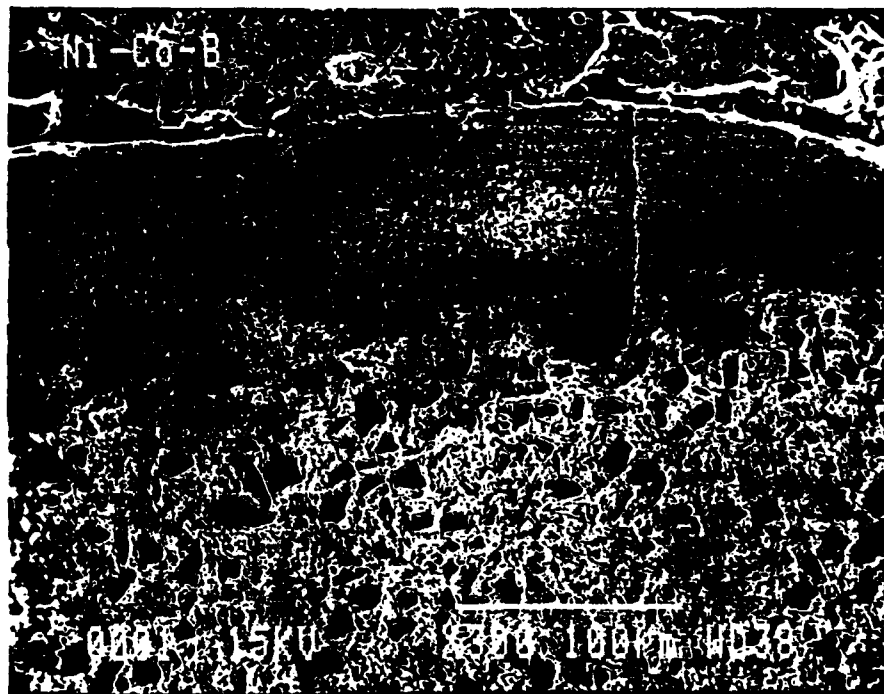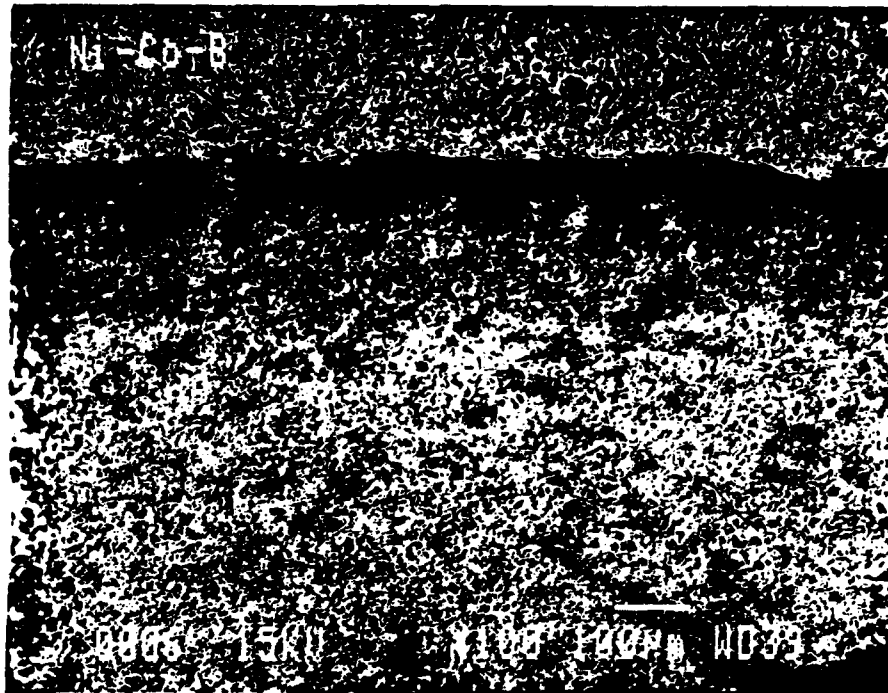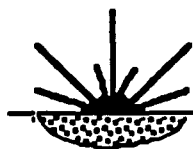
Figure 10. Scanning electron micrographs of laser glazed Al/SiC predeposited with salt precursors of Ni, Co and B (Laser power 1500 watts) showing the uniform glassy-like layers. (a) Mag. 100x, (b) Mag. 300x.

Table 6. Microhardness Data of Ni-Cr-Co-B Laser Coatings

Scan Rate mm/sec	Average Coating Thickness, microns	Hardness Readings, HV
42	30	110 *, 130*
34	50	270, 280, 290, 400
25	75	210, 245, 290, 400
17	100	330, 670, 1200, 1700
Substrate		77, 80, 85, 90, 95

* Indentations were mostly on the substrate

4.9 Tribological Behavior

Friction and wear tests were conducted using the well known Pin-on-Disk test rig. The sliding system consisted of laser coated Al/SiC (disk) and a hardened 52100 steel pin(6 mm diameter, 25 mm long). The wear test parameters are given in Table 6. No lubricant was added and the humidity was controlled to 60 %. The additive weight loss of the disk was measured to determine the wear using a precision balance to an accuracy of 10^{-5} gms. Wear tests were also carried out using 6061 -Al alloy and uncoated Al/SiC as disks for comparison purposes.

Figure 18 provides the weight loss as a function of sliding time for Al/SiC, laser coated Al/SiC with Ni-Cr-Co-B and 6061-T6 aluminum. It is seen that the uncoated Al/SiC wears out linearly with time and also has excessive wear when compared to laser coated Al/SiC. Laser coated sample exhibited higher wear rate initially due to the presence of loose oxides and surface roughness. After "Running-in" wear, the wear rate becomes negligible. Such wear behavior is not observed in 6061-T6 aluminum and uncoated Al/SiC samples. This clearly indicates that the laser coating has the superior capability to enhance the wear resistance.

Friction data plotted in Figure 19, shows that the steady state friction for laser coated sample is the same as that of the substrate. To correlate friction and wear, and to identify the friction and wear mechanisms of laser coated samples, a detailed analysis of worn surfaces is required and will be performed in Phase II.
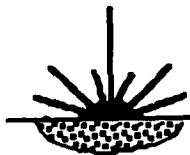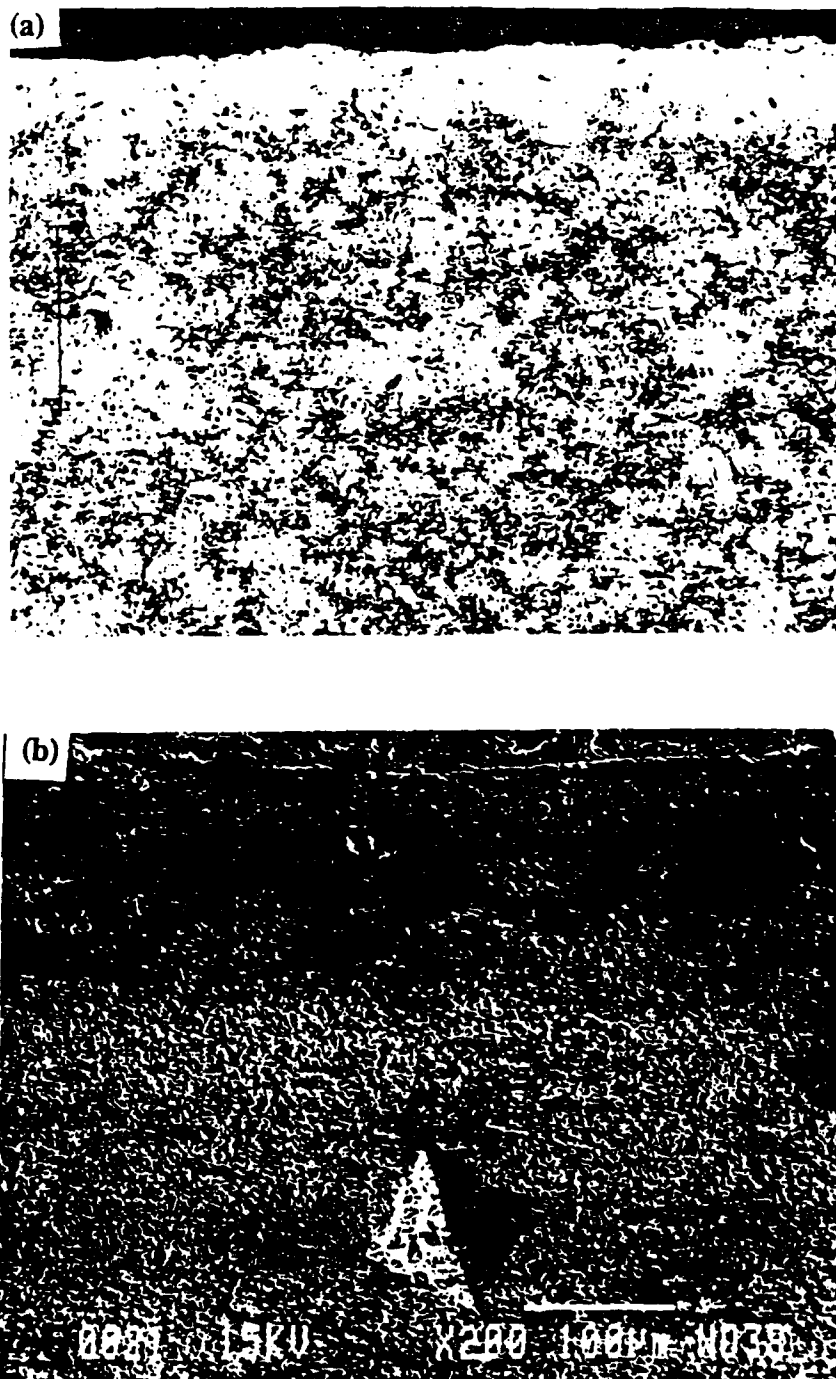
Figure 11. Micrographs of laser glazed Al/SiC predeposited with
Ni, Co, Cr and B salt precursors showing the uniform amorphous-
like coating. (a) Optical micrograph, Mag. 50x, (b) Scanning
Electron Micrograph, Mag. 200x.

Ni-Co-Cr-B sample

Vert.= 500 counts Disp= 1

Preset= 150 secs
Elapsed= 150 secs

0.000 Range= 10.230 keV 9.470

Si

Al

Co

Ni

O

Cr

Co Ni

Ni
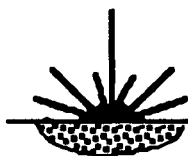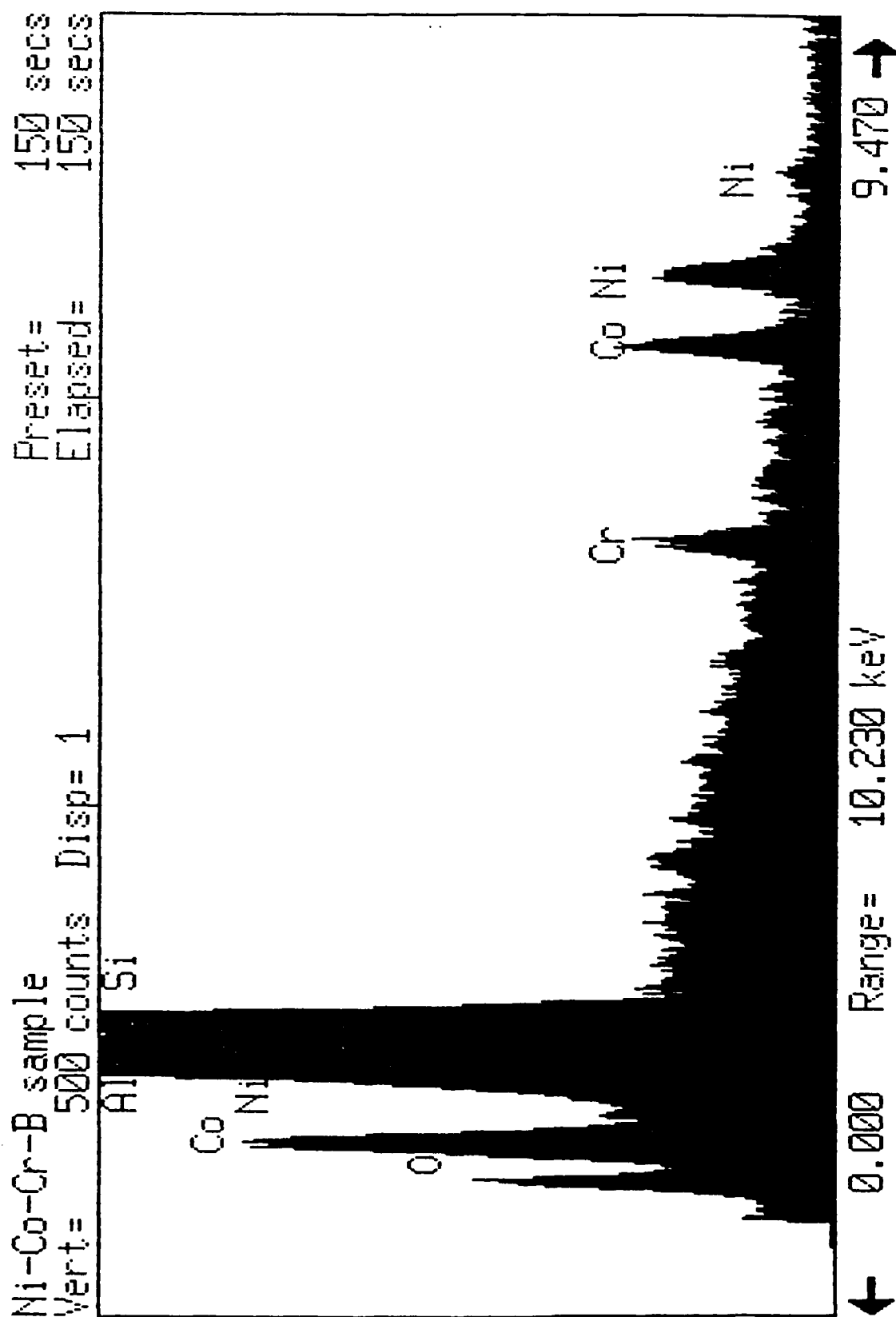
Figure 12. X-Ray Energy Spectrum of Laser Glazed Ni-Cr-Co-B system on Al/SiC Composite.
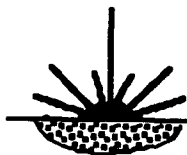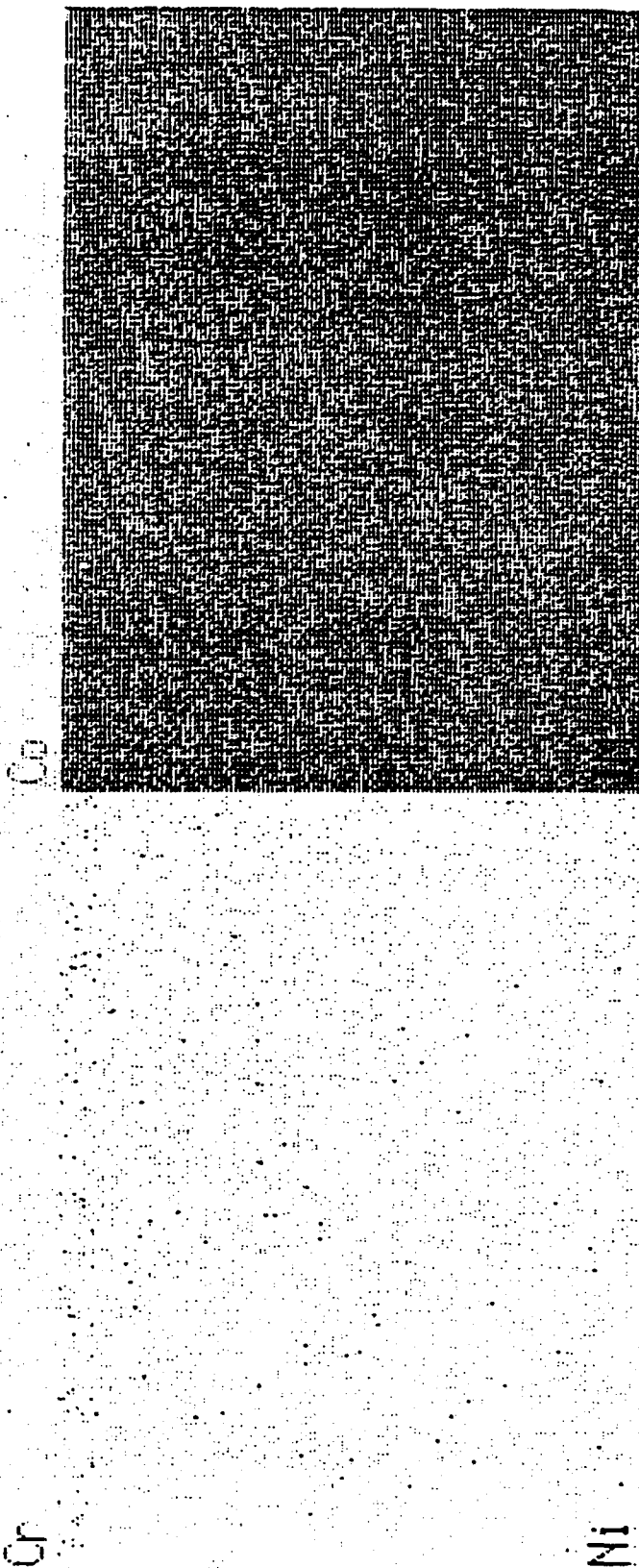
Figure 13. Scanning electron image of laser glazed Ni-Cr-Co-B coating and X-ray dot mapping of Ni, Cr, and Co showing a homogeneous distribution of the elements, Mag. 1000x.
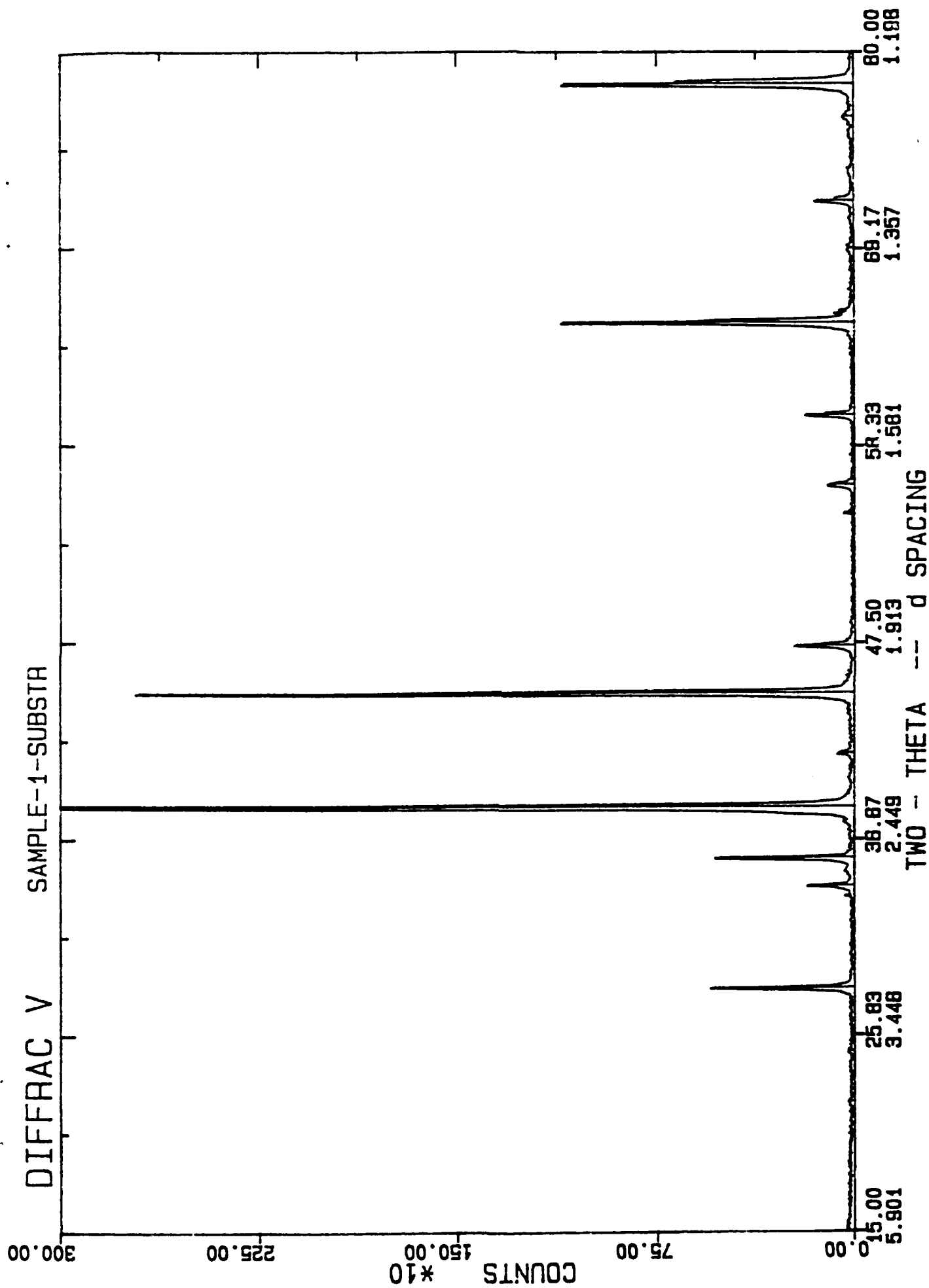
Figure 14. X-Ray Diffractogram of Al/SiC Composite Substrate.

24
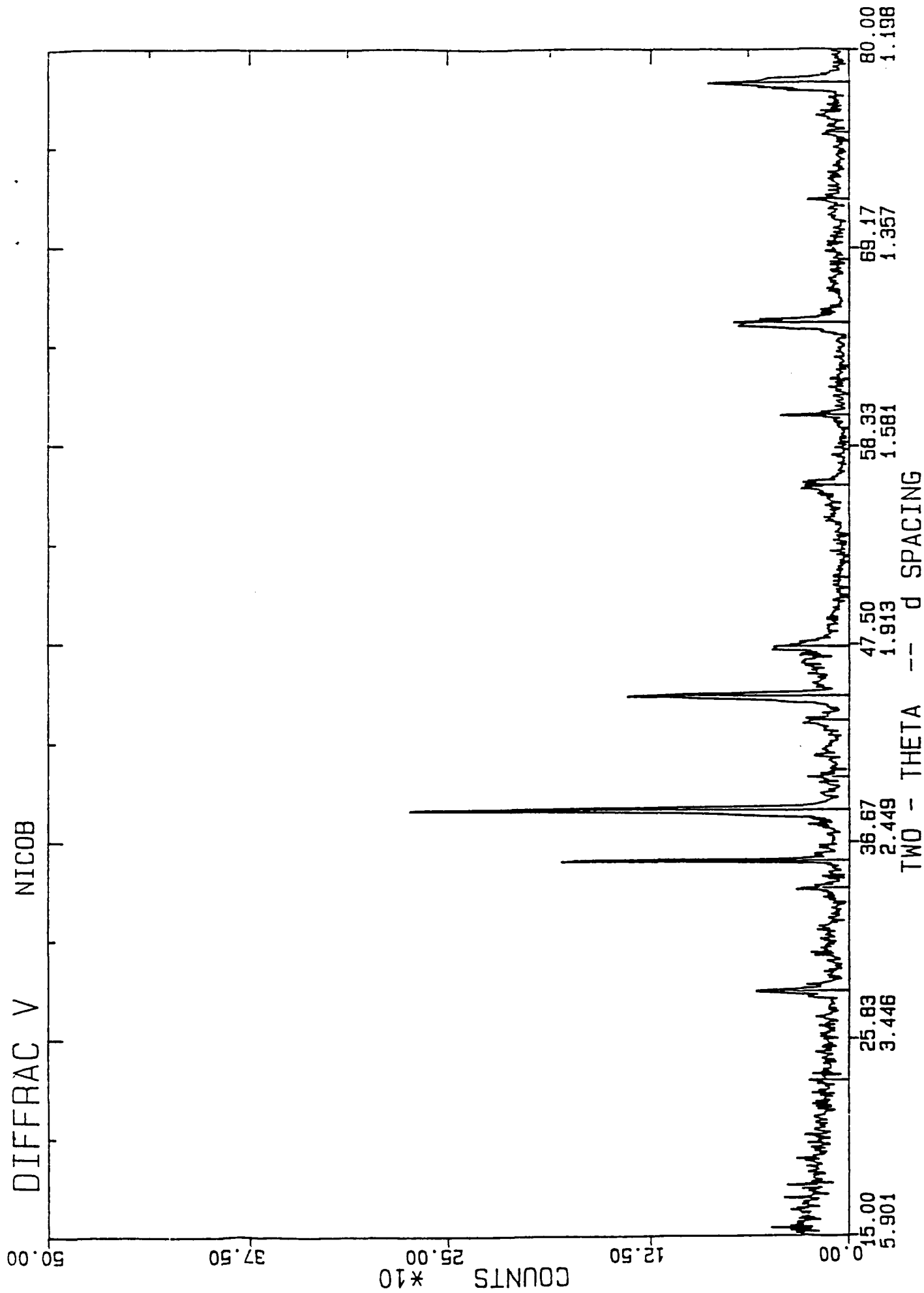
Figure 15. X-Ray Diffractogram of Laser Glazed Ni-Co-B on Al/SiC.

25
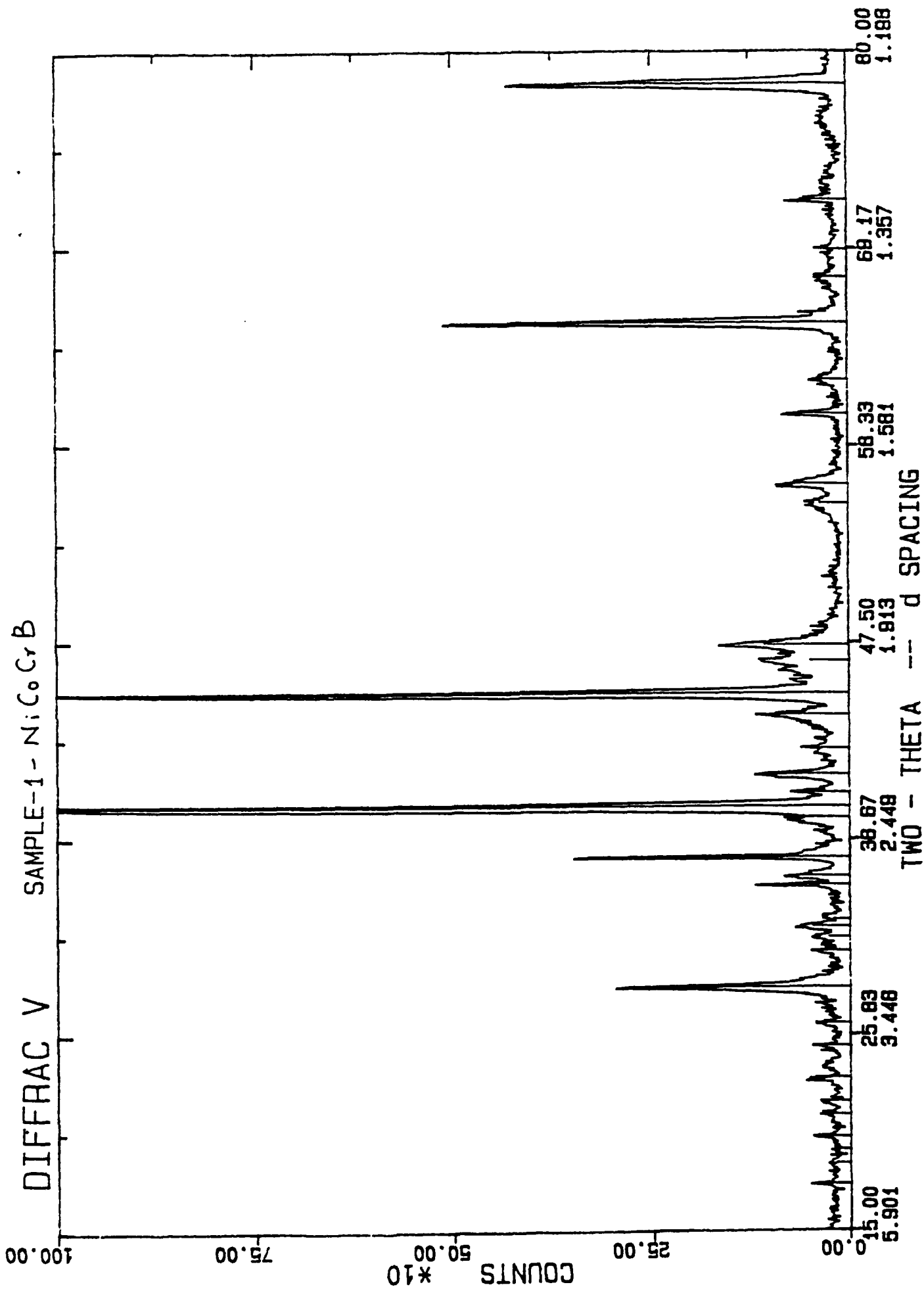
Figure 16. X-Ray Diffractogram of Laser Glazed Ni-Co-Cr-B on Al/SiC.
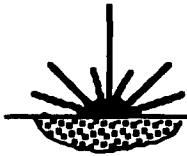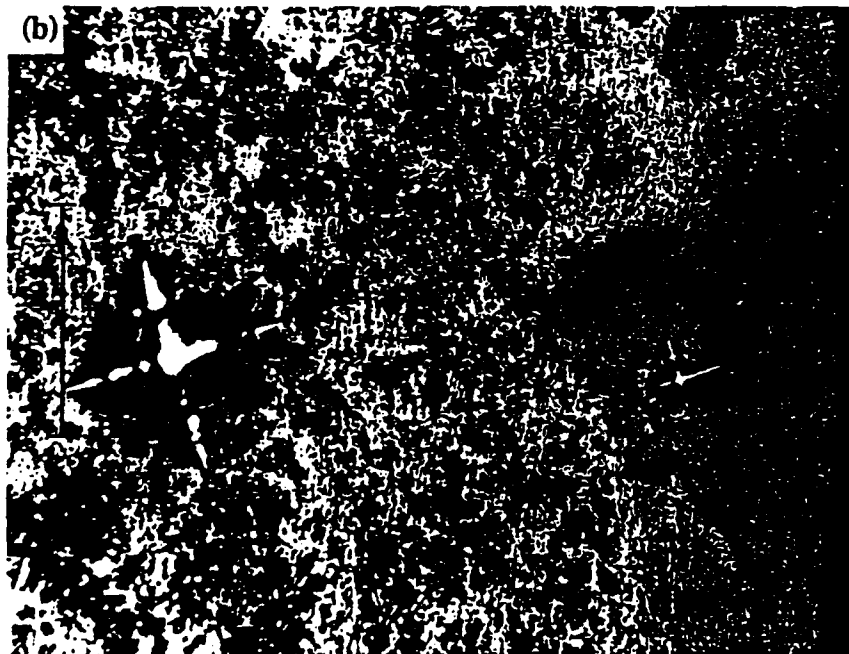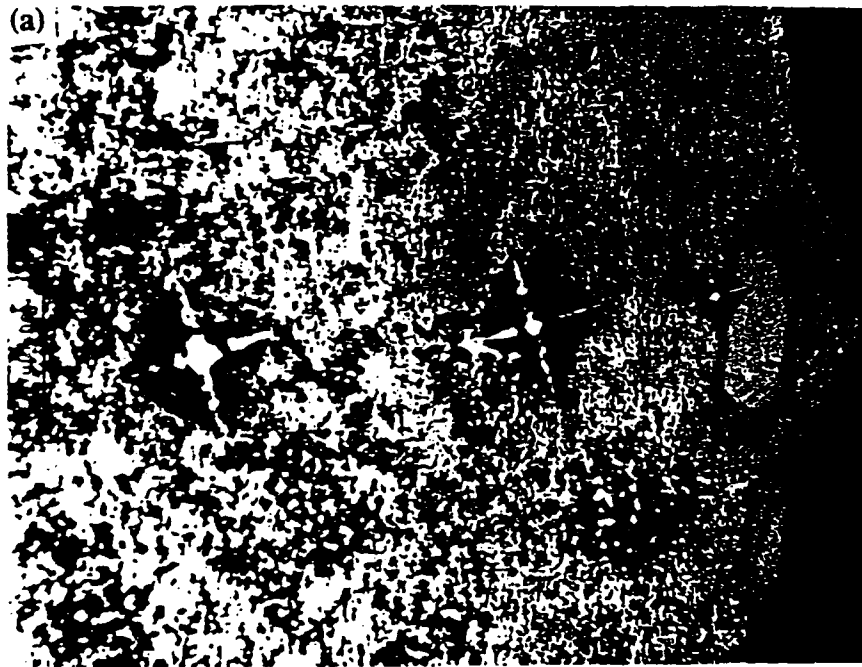
Figure 17. Optical micrographs of laser glazed Ni-Cr-Co-B coating showing the Vicker's hardness indentations on the coating and substrate.
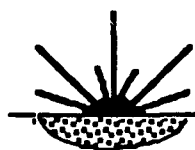
Table 7. Sliding Wear Test Conditions and Parameters

Pin	Hardened 52100 Steel	(60-64 Rc)
Disk	Al/SiC substrate	(80-90 HV)
	Laser coated Al/SiC	(300-1700 HV)
	6061-T6 aluminum	(100-110 HV)
Load	10 Newtons	
Velocity	0.183 m/sec	
Diameter of track	10 mm	
Sliding time	upto 5 hours	
Temperature	Ambient	

4.10 Evaluation of Corrosion Resistance by Anodic Potential Test

For corrosion testing, lacquer was applied on all sides of the sample except on the laser treated face, leaving an exposed area of about 13,225 mm^2 for electrochemical test. The electrolyte used was aerated (open to air) 0.1 N NaCl. The experimental procedure involved recording open-circuit potential with the time of immersion and monitoring current-potential relationships using potentiodynamic polarization technique. The samples were immersed in electrolyte until a steady open-circuit potential (E_{corr}) was recorded (approximately for 1 hour). After this time the potential was increased at a rate of 0.5 mv/sec. Potentiodynamic polarization curves were recorded with an EG & G PAR Model 273 Potentiostat/Galvanostat controlled by an external microcomputer.

The anodic polarization curves (Figure 20) shows that the open-circuit potential for the laser coated and uncoated samples was almost identical. The open-circuit potential for laser coated specimen was initially lower and then fluctuated with time. In contrast, the open-circuit potential for uncoated specimen was initially higher and then decreased with time (Figure 20a). After an hour, the corrosion potential for both specimens was stablized due to the formation of a passive film. E_{corr} values for uncoated sample and coated samples were -0.6260 and -0.6200 volts respectively. However, the anodic current density for a given potential is lower for laser coated Al/SiC implying the less susceptibility to pitting corrosion. The plot shows that the laser coated samples are more passivated with increase in applied potential.

4.11 Laser Coating of Al/B₄C Composites

The laser glazing process involving laser chemical reduction of Ni-Cr-Co-B salts was also applied to produce amorphous coatings on Al /B4C composites. The composite was obtained from Fiber Materials Inc., Space Technology Division, Columbus, Ohio, and is a particulate reinforced composite containing 50 vol% B₄C in 6063 aluminum matrix. Figure 21 is scanning electron micrograph showing the boron carbide particles in the matrix.
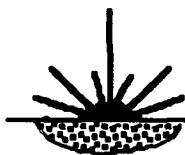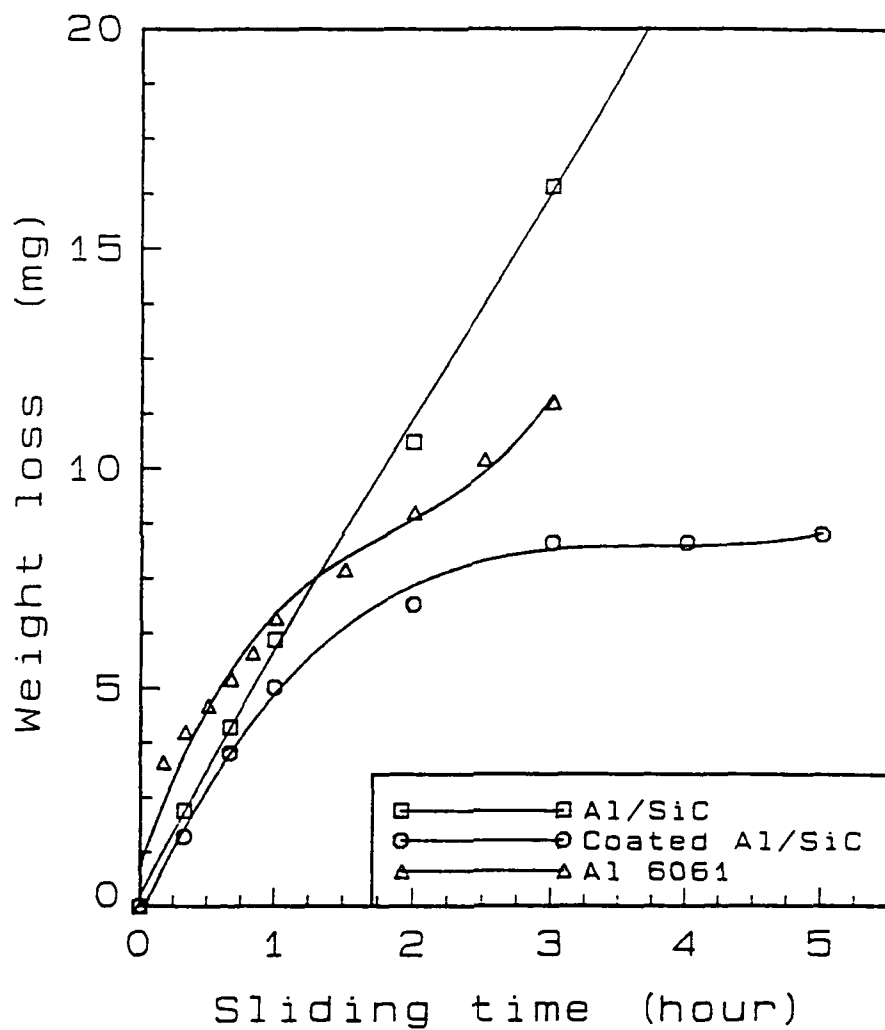
Figure 18. Sliding wear behavior of Al/SiC, laser coated Al/SiC
and 6061-T6 aluminum.
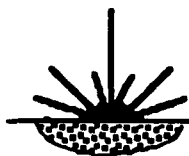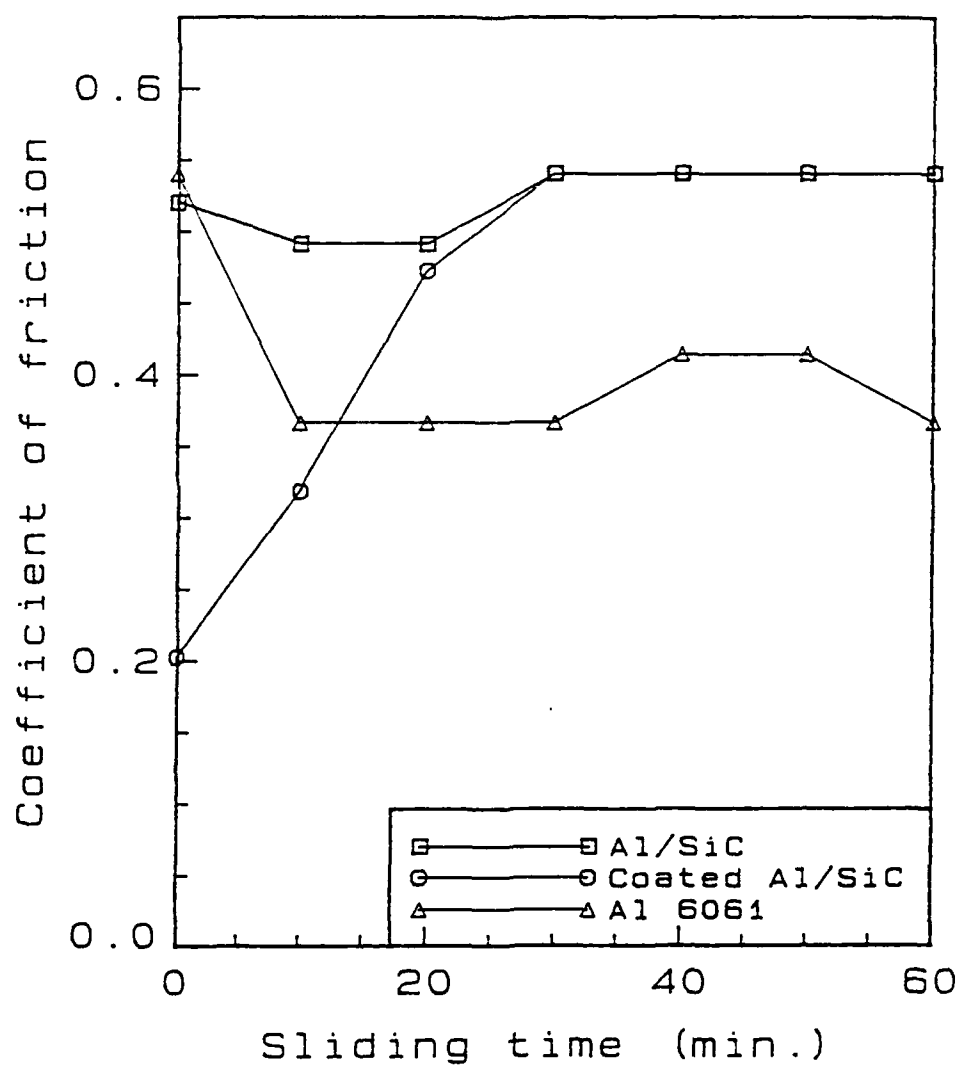
Figure 19. Friction behavior of Al/SiC substrate, laser coated Al/SiC and 6061-T6 Al.
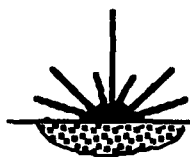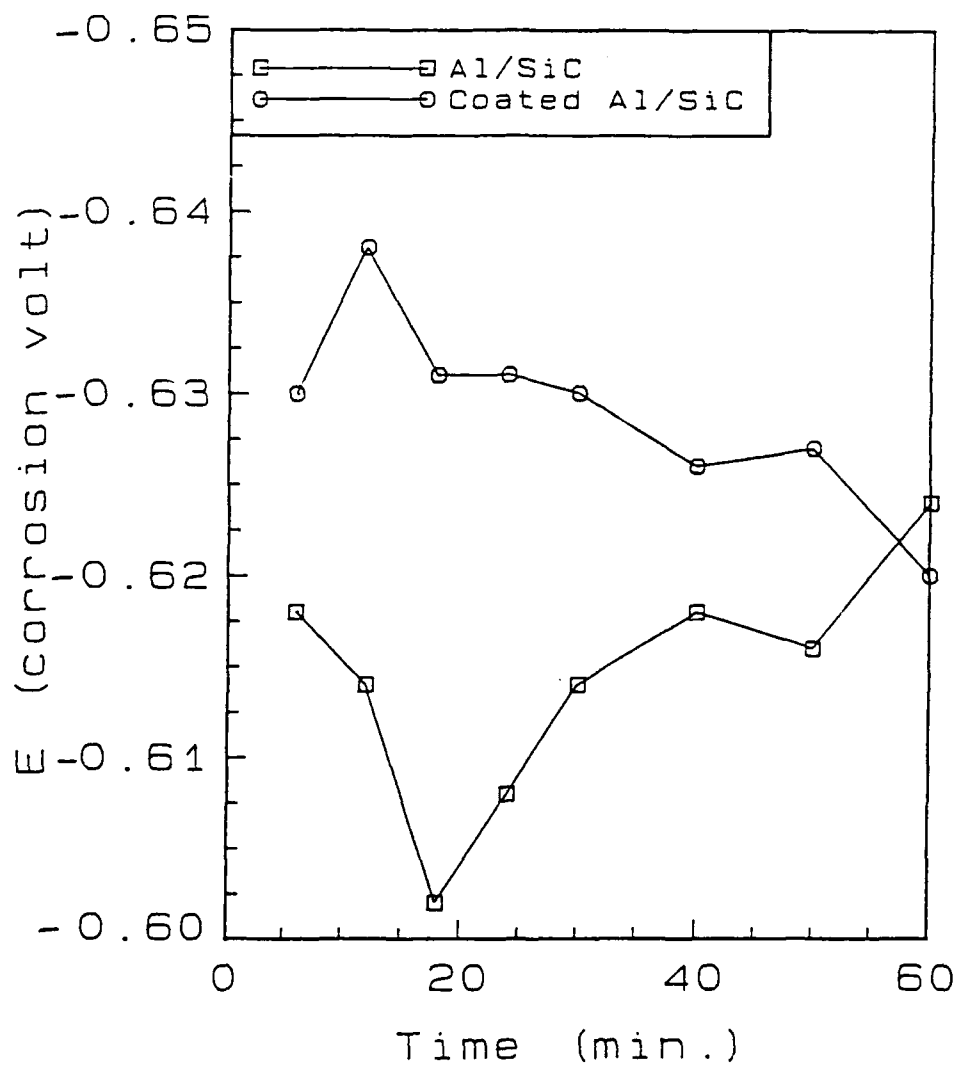
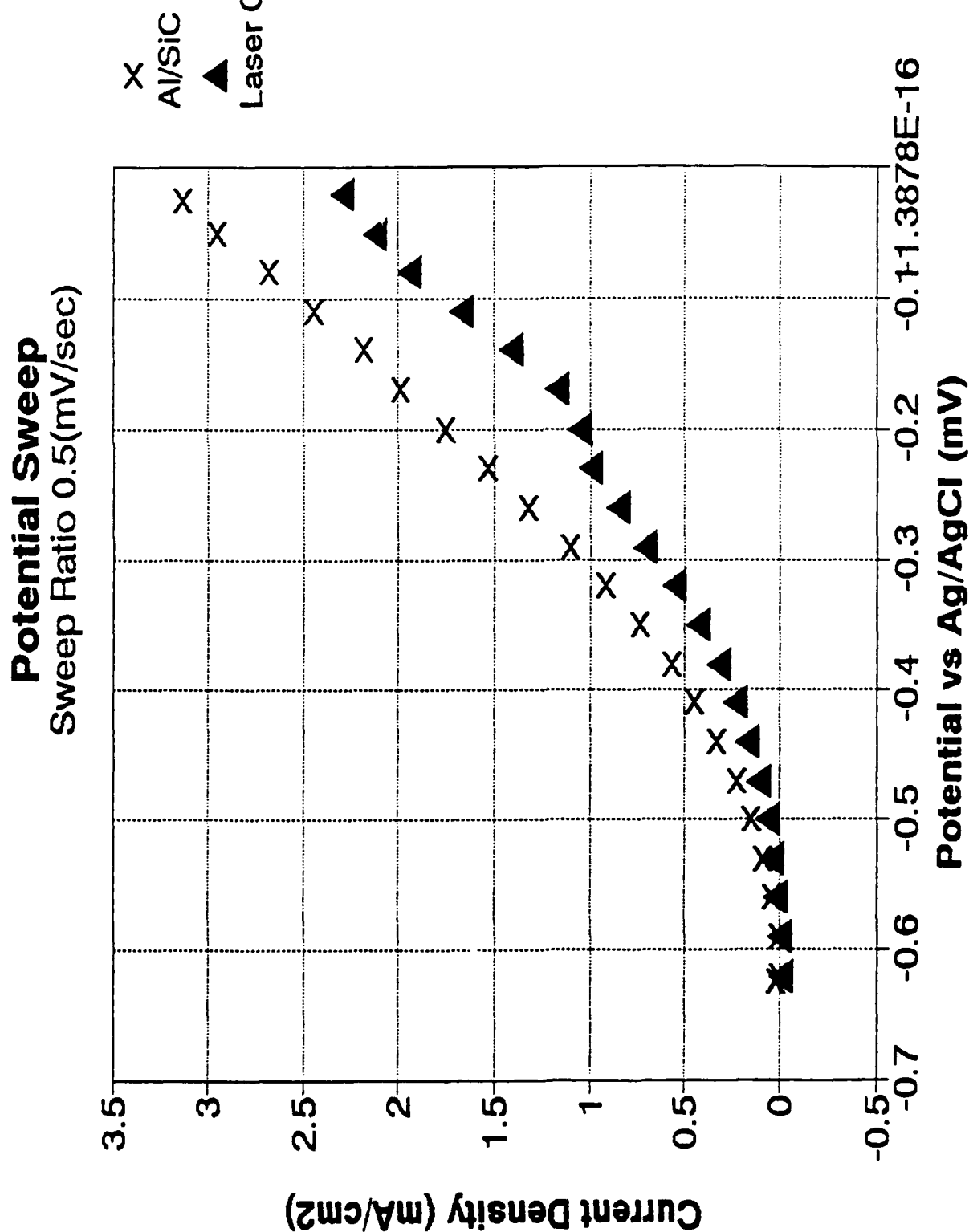Figure 20a. Open-circuit potential as a function of time in 0.1N
NaCl solution for laser coated Al/SiC and the uncoated Al/SiC
specimen.
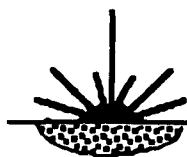
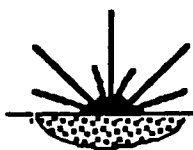Figure 20. Potentiodynamic Polarization Curves for Al/SiC substrate and Laser Coated Al/SiC in 0.1 N NaCl solution.

Figures 22 and 23 are transverse sections of the laser coated specimen showing an uniform coating with a nominal thickness of 60 microns. Detailed scanning electron microscopical analysis at higher magnifications did not reveal any crystalline microstructures (Figure 24). The microhardness data indicated that the coating had a hardness in the range of 260-400 HV (substrate hardness: 300-500 HV). But a remarkable increase in the hardness was noted at the coating-substrate interface, which ranged from 1200-1400 HV. This shows significant increase in the bonding strength of the coating to the substrate.

The coatings obtained on Al/B$_4$C composites exhibit better characteristics than the coatings on Al/SiC.

* The coatings appear to be more amorphous-like possibly due to the presence of boron in the substrate.

* The coatings are much more uniform with a distinct interface between coating and substrate.

* Microhardness at the coating-substrate interface is very high, showing good bonding.

4.12 Eddy Current NDE Evaluation of Laser Coatings

Eddy current NDE (ECNDE) is a viable technique for evaluating the glassy surface layers of laser coated components becuase it is sensitive to the variations in the electrical and magnetic properties of the surface layers (10). The glassy layers generally exhibit higher magnetic permeability than the crystalline counter parts. ECNDE is also an effective on-line monitoring tool for determining the thickness and probing the defects, such as porosity and cracks. The eddy current probe generates a magnetic field which induces eddy current in the specimen, and these eddy currents generate their own magnetic field which interacts with the probe's magnetic field. The complex phase/amplitude (phasor) interactions of these two magnetic fields leads to changes in the phase and amplitude of the probe's impedance. The probe impedance depends on the electrical conductivity and magentic permeability of the surface layers. The impedance consists of two orthogonal components; resistive and reactive.

We have used ECNDE technique on laser glazed Al/SiC and Al/B4C composites. Figure 25 displays an automated eddy current measurement system used in this study. Measurements of the probe impedance were accomplished with a precision impedance analyzer (HP4194A). A computer-controlled X-Y positioning stage permitted one or two-dimensional scans of the specimens. The real (Resistive) and imaginary (Reactive) parts of the probe impedance were recorded at 1 MHz. The spacing (lift-off) between the probe and surface was 0.15 mm.
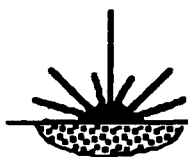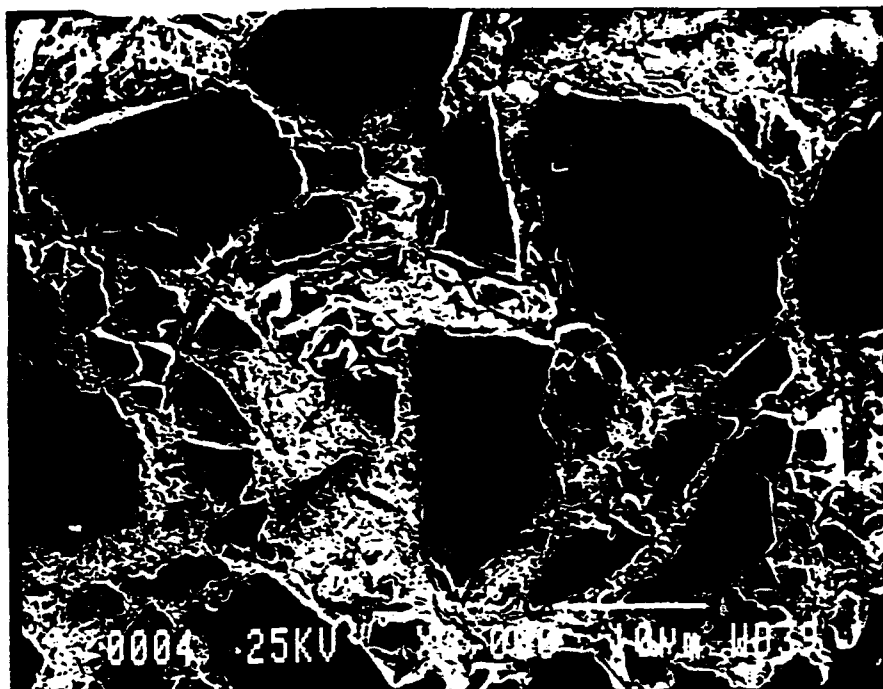
Figure 21. Scanning electron micrograph of aluminum/boron carbide composite showing the particle size and distribution of carbide particles, Mag. 2000x.
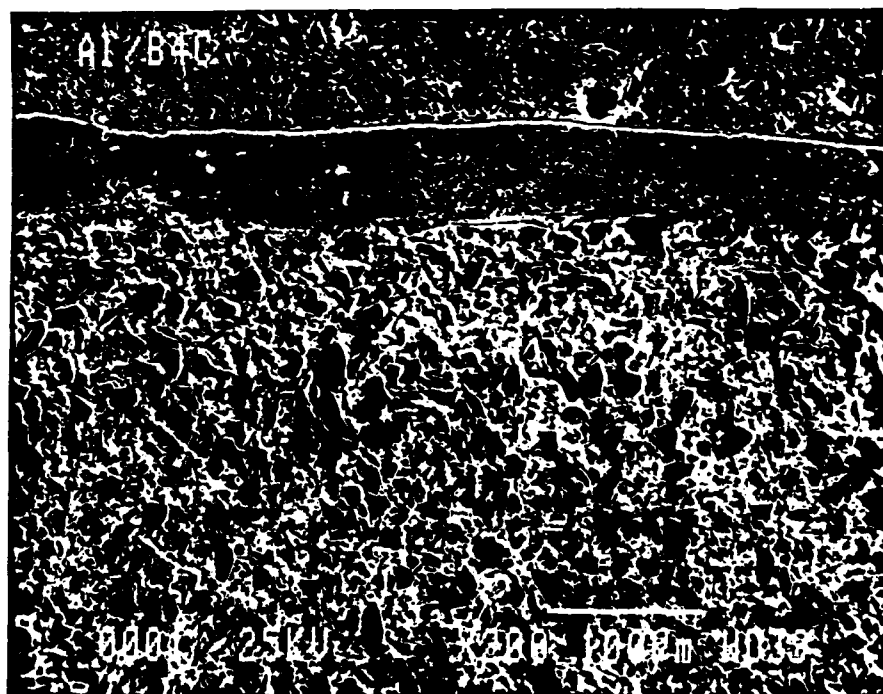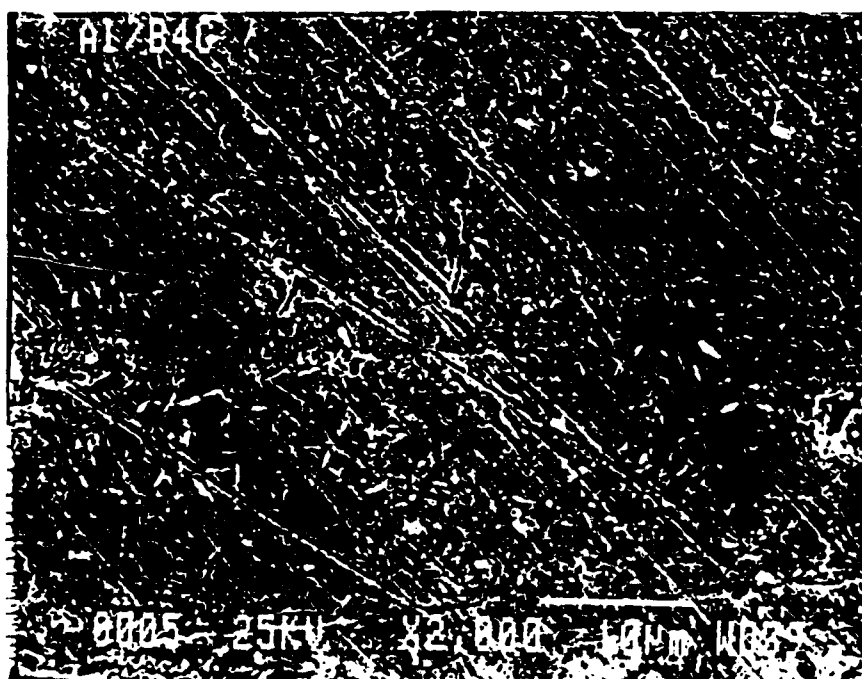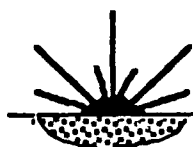

Figure 22. Scanning electron micrograph of laser glazed Al/B4C predeposited with Ni, Cr, Co and B salt precursors showing the uniform amorphous-like coating, Mag. 200x.

Figure 23. Scanning electron micrograph of laser glazed Al/B4C predeposited with Ni, Cr, Co and B salt precursors showing the uniform amorphous-like coating, Mag. 500x.

Figure 24. Scanning electron micrograph of laser glazed Al/B$_4$C predeposited with Ni, Cr, Co and B salt precursors showing the uniform amorphous-like coating, Mag. 2000x.
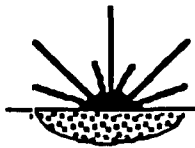
Automated Eddy Current Measurement System

Figure 25. Schematic diagram of automated eddy current measurement system.

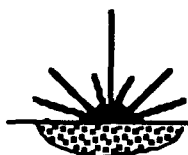Figures 26 to 27 are the results of ECNDE of laser coated and uncoated composites. The lower resistance and higher reactance of the laser coated layers imply the possibility of formation of glassy layers. The impedance signal distributions shown in Figure 28 indicate the formation of laser coated layers. The presence of glassy-like coatings in the laser scans can be distinguished very clealy in the laser coated samples (Figure 28b). The phase angle of the eddy current probe impedance is higher for laser coated (83.00 degrees) than uncoated samples (82.60 degrees) which can also be used to identify the presence of coated glassy layers.

Generally ECNDE techniques are used to detect the flaws-surface cracks, voids, inclusions, etc.-during manufacturing and service. In our work we intend to use this technique to identify the glassy layers and measure coating thickness. Since it is a non-contact method, it is ideally suitable for on-line monitoring during laser glazing process. The impedance analyzer used in our experiment permits quantitative measurements of the probe impedance over a range of frequencies, which is not possible with commercially available eddy current instruments. With proper calibration, the use of frequency-dependent eddy current measurements can be used to determine the thickness and conductivity of glassy layer coatings on composite materials.
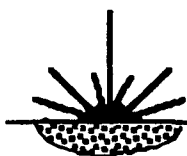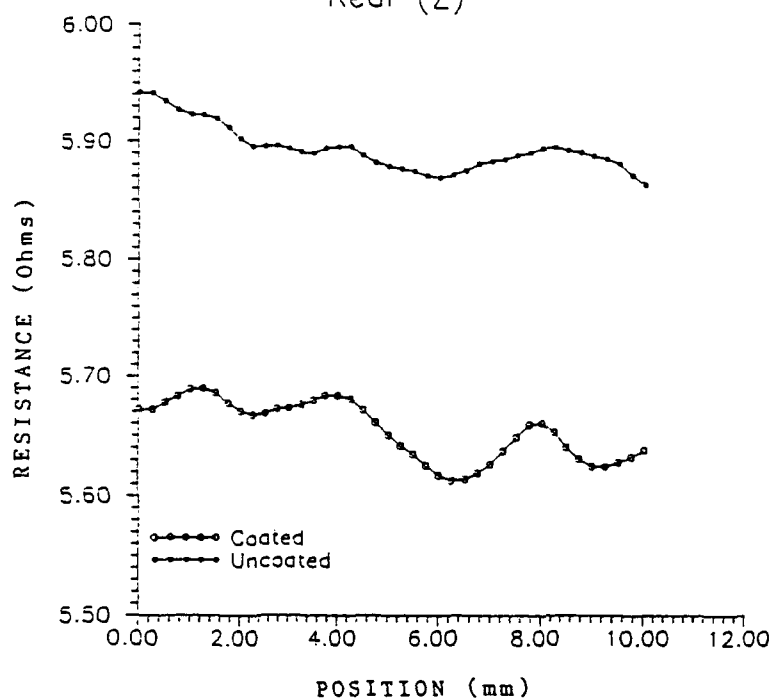
Applications in Materials Development

Aluminum—SiC
Real(Z)

(a)
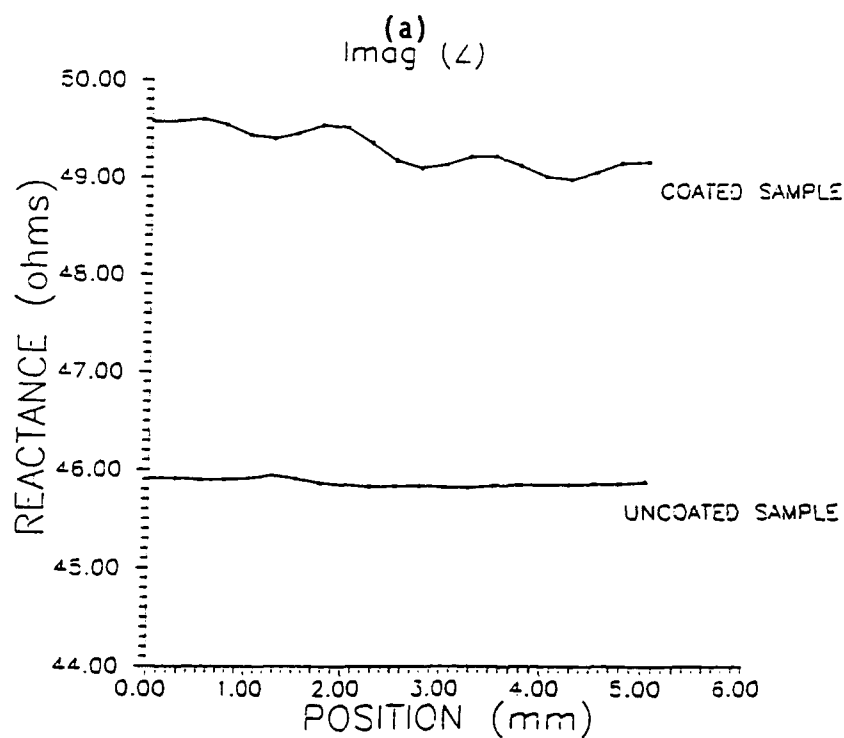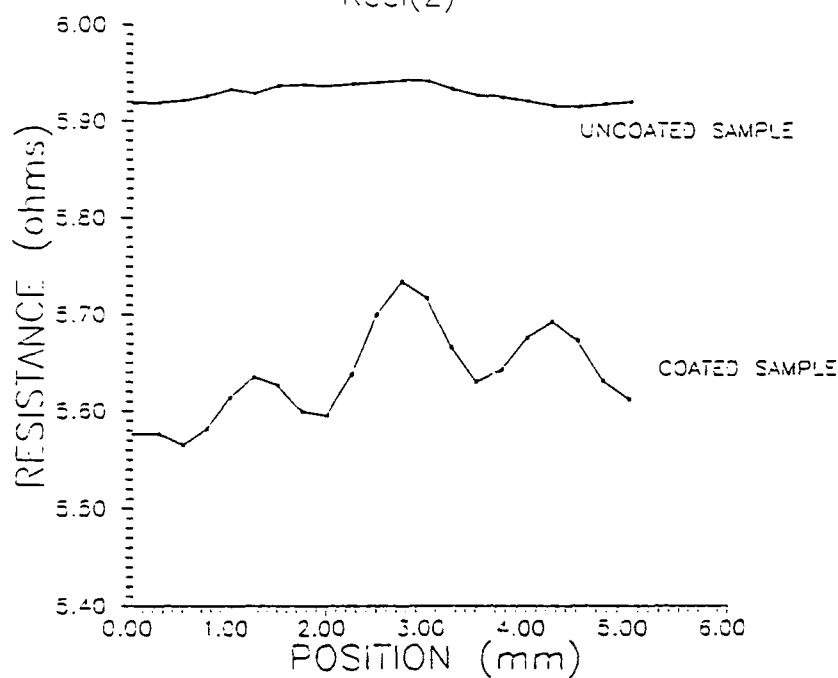
Imag (Z)

(b)

Figure 26. Measurements of impedance during 2-d scanning of Al/SiC sample: (a) Real part (Resistance) change (b) Imaginary part (Reactance) change.
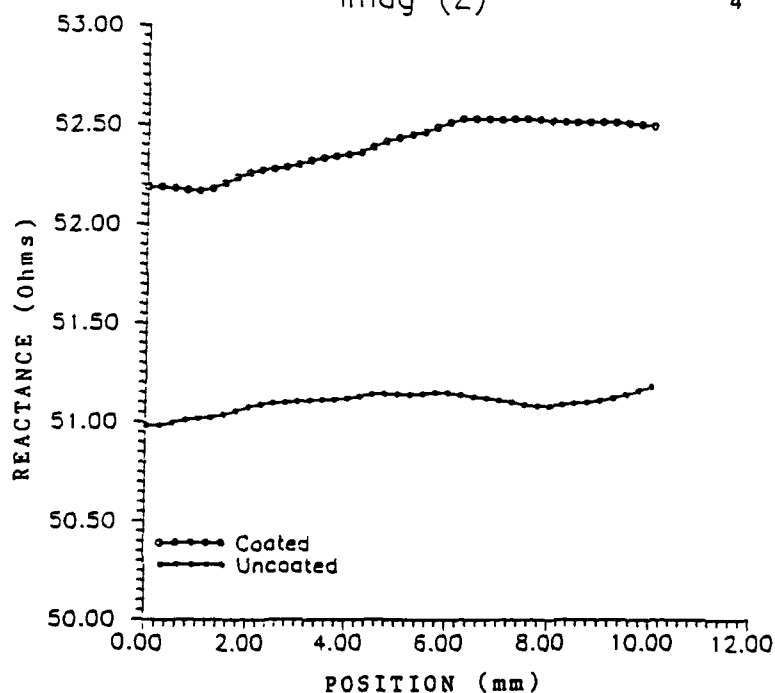
Real (Z) Al/B_4C
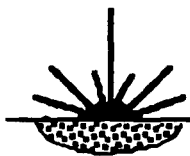

(a)

Imag (Z) Al/B_4C

(b)

Figure 27. Measurements of impedance during 2-d scanning of
Al/Boron carbide sample: (a) Real part (Resistance) change
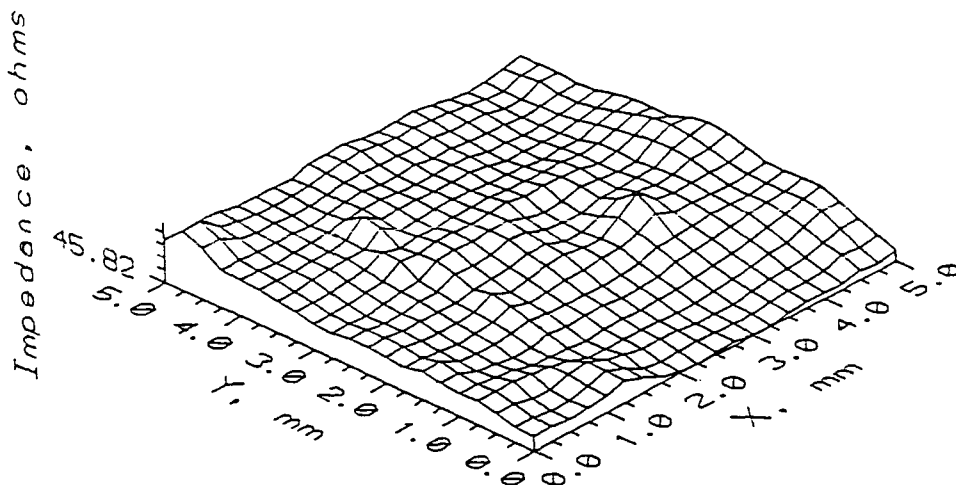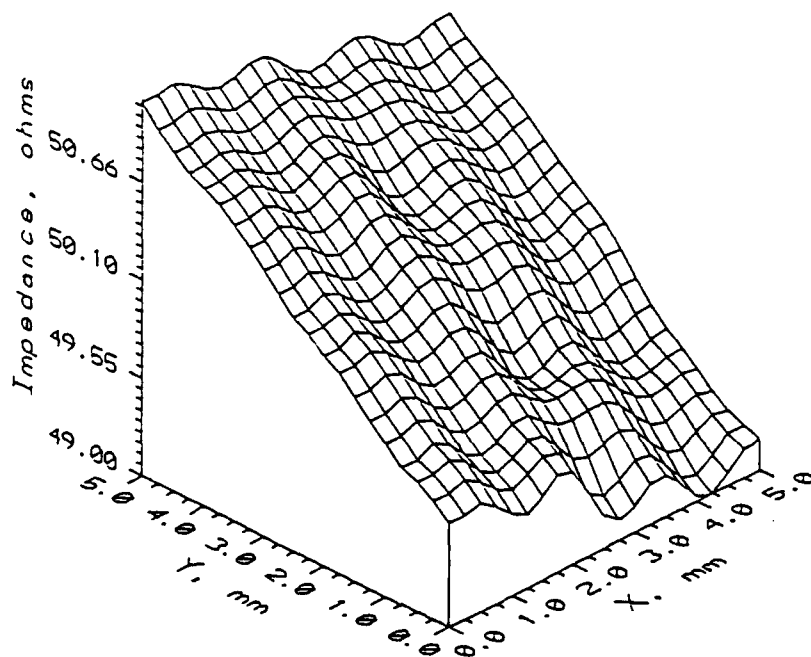(b) Imaginary part (Reactance) change.

UNCOATED Al/SiC sample
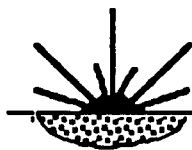
(a)

Coated Al /SiC

(b)

Figure 28. 3-D plots of impedance signal distribution
in uncoated and coated samples of Al/SiC.

5. ANTICIPATED BENEFITS TO DoD

Space structures including structures for prime power systems, antennas, tracking and pointing systems, solar collectors and pressure vessels pose many design problems in terms of stiffness, fatigue resistance, impact resistance, high temperatures, corrosion resistance and tribological properties. Most of these space structures are made of MMCs. Proposed research has significant potential in improving the performance of these composites in aggressive space environment and is capable of improving the fatigue resistance and damage tolerance. An area of great interest in MMCs is the development of high-temperature composites for applications in the extreme environment of the NASP. The formation of glassy coating by the process developed in Phase I research will improve the oxidation, corrosion, and wear resistance of these materials. The success of this project will enable us to obtain glassy coatings on MMCs by a process which is simple, versatile, and which does not require any vacuum or inert atmospheres. The process cal be carried out at higher speeds and also can be automated.
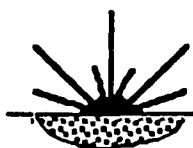
6. CONCLUSIONS

Phase I research indicates that laser glazing technique using the salt precursors is a viable and effective method for depositing complex composition coatings on advanced composites. Although a comparison with other coating methods such as CVD, sputtering etc has not been made to date, the laser coating process developed in Phase I offers several benefits that include:

1. Synthesis of amorphous-like microstructures and enhancement in hardness, wear and corrosion resistance of metal matrix composites indicating that laser coating process may be technically superior than other methods for providing oxidation, wear and corrosion resistance.

2. The process is versatile. Any combination of elements and compounds can be deposited on the substrate.

3. The process is simple. There is no need for vacuum or inert atmosphere. Preheating of the substrate is not required to perform the coating operation.

4. The process can be carried out at much higher speeds than many other coating processes.

5. The process is adaptable for automation which in turn will allow coating large scale structures and complex shaped components.
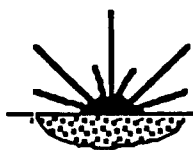
A major benefit of using laser coatings is the conservation of strategically important elements such as Co, Cr, and Ni. Laser processing is generally better than other conventional methods essentially due to the rapid solidification effects leading to glassy and other nonequilibrium microstructures. For example, laser deposited Cr-coatings can exceed the wear and corrosion performance of electroplated Cr-coatings. Annually, about 10 million kilograms of chromium are consumed just in Cr-plating. Laser coating procedure can not only bring down this figure but will also reduce the environmental problems associated with Cr-plating. It should be added that a laser beam, being a clean source of energy, can drastically reduce the pollution problems associated with many techniques. Laser coatings can have potential impact on energy conservation through reduced friction, system reliability and overall productivity enhancement.

REFERENCES

1. Current Highlights, Publications of the Metal Matrix Composite Analysis Center, 6, 3, Santa Barbara, CA, 1986, 1.

2. A. Mortensen, J. Cornie and M. Flemings, J. Metals, Vol. 40, 2, 1988, 12.

3. M. Hunt, Materials Engineering, November 1990, 35-38.

4. M. D. Archer, C. C. Corke and B. H. Harji, Electrochimica Acta, Vol. 32, 1, 1987, 13-26.

5. E. J. Kubel Jr., Metal Progress, May 1986, 61-70.

6. B. H. Kear, E. M. Breinan and L. E. Greenwald, Metals Technology, April 1979, 121-129.

7. H.W. Bergmann, B. L. Mordike, J. Materials Science, Vol. 16, 1981, 863-869.

8. K. Hashimoto, N. Kumagai, H. Yoshika and K. Asami, Materials and Manufacturing Processes, Vol. 5, 4, 1990, 567-590.

9. N. Kumagai, K. Asami and K. Hashimoto, J. Non-Crystalline Solids, 87, 1986, 123-136.

10. R. J. Churchill, J. M. Glass, H. P. Groger and S. S. Lane, SPIE Vol. 952, Laser Technologies in Industry, 1988, 334-339.